CENTRO DE INVESTIGACIÓN Y DE ESTUDIOS AVANZADOS DEL INSTITUTO POLITÉCNICO NACIONAL

Unidad Mérida

DEPARTAMENTO DE FÍSICA APLICADA

"*Reaction Force*: a Module to Analyze Chemical Properties through the Intrinsic Reaction Coordinate"

a thesis submitted by

Alan Israel Quintal Flores

In partial fulfillment of the requirements for the degree of

Master of Science

in

Physical Chemistry

Thesis Advisor:

Dr. José Gabriel Merino Hernández

Mérida, Yucatán, México August 2020

CENTRO DE INVESTIGACIÓN Y DE ESTUDIOS AVANZADOS DEL INSTITUTO POLITÉCNICO NACIONAL

Unidad Mérida

DEPARTAMENTO DE FÍSICA APLICADA

"*Fuerza de Reacción*: un Módulo para el Análisis de Propiedades Químicas a lo largo de la Coordenada Intrínseca de Reacción"

TESIS

Que presenta

Alan Israel Quintal Flores

Para obtener el grado de

Maestro en Ciencias

en

Fisicoquímica

Director(es) de Tesis:

Dr. José Gabriel Merino Hernández

Mérida, Yucatán, México Agosto de 2020

ACKNOWLEDGEMENTS

I would like to express my deepest appreciation…

To my parents, for their love and support throughout my life. Thank you for being my cornerstone.

To my thesis advisor, Dr. Gabriel Merino, who provided me with encouragement and support throughout this project, and allowed me to work in something I love, programming.

To M. S. Eugenia Dzib, who provided me with her experience and knowledge to the development of this project.

To my committee, for their time and dedication in reviewing my thesis.

To Dr. Alejandro Estrella, who has been a mentor, a friend, and an inspiration to my professional and academic life.

To all my master colleagues and friends, Raúl, Silvana, Carlos, Gregorio, Jair, Gabriela, and Luis, with whom I have shared moments of anxiety but also of excitement. Their presence makes these last two years an amazing experience.

To my friends Gabriela, Rossana, Angie, Karla, and Eduardo for your words of support in the most difficult moments, despite the distance.

To Conacyt for the financial support provided during the master's studies.

Thank you all for believing in me.

INDEX

LIST OF ABBREVIATIONS

Abbreviation	Explanation
DFT	Density Functional Theory
DA	Diels-Alder
DGT	Double Group Transfer
HF	Hartree-Fock
HOMO	Highest Occupied Molecular Orbital
IRC	Intrinsic Reaction Coordinate
LUMO	Lowest Unoccupied Molecular Orbital
MEP	Minimum Energy Path
NBO	Natural Bond Orbital
NIST	National Institute of Standards and Technology
ODE	Ordinary Differential Equation
PES	Potential Energy Surface
RP	Reaction Path
SDRP	Steepest Descent Reaction Path
TS	Transition State
WBI	Wiberg Bond Index

ABSTRACT

Reaction force module, written in *Python*, has been implemented in the *Eyringpy Program* to compute the reaction force, reaction force profiles, and energy decomposition into the three stages proposed by Toro-Labbé, and to perform structural and electronic properties analysis along the intrinsic reaction coordinate. An interpolator has been implemented, to smooth the potential energy, reaction force, and reaction force constant profiles. One of the advantages of this module is that a complete analysis of a reaction mechanism can be performed in a short time. Four pericyclic systems have been chosen to validate the module: the Diels-Alder reaction between *s-cis*-butadiene and ethylene, the electrocyclization of 1,3,5-hexatriene to 1,3-cyclohexadiene, the degenerate [3,3] Cope rearrangement of 1,5-hexadiene, and the double group transfer between ethane and ethylene.

RESUMEN

El *módulo de la Fuerza de reacción*, escrito en *Python*, ha sido implementado en el programa *Eyringpy*, para el cálculo de perfiles de fuerza, constante de fuerza de reacción, la descomposición de energía en los tres estados propuestos en el modelo de Toro-Labbé y el análisis de propiedades estructurales y electrónicas a lo largo de la coordenada intrínseca de reacción. Un interpolador ha sido implementado en este módulo para suavizar las curvas de energía, fuerza de reacción y constante de fuerza de reacción. Una de las ventajas de este nuevo módulo es que el tiempo de cómputo es corto. Cuatro reacciones pericíclicas han sido elegidas para validar este módulo: la reacción Diels-Alder entre *s*-*cis*-butadieno y etileno, la electrociclización de 1,3,5-hexatrieno a 1,3-ciclohexadieno, el rearreglo de Cope del 1,5-hexadieno y la doble transferencia de protones entre etano y etileno.

INTRODUCTION

"…science is the most revolutionary force in the world."

- George Sarton[1]

Understanding a chemical reaction involves the knowledge of its mechanism. Despite activation barriers describing the kinetics or reaction energies reflecting thermodynamic aspects, identifying physical and chemical properties along the reaction path contributes primarily to the overall understanding of reaction mechanisms.[2] Real knowledge of a reaction mechanism involves a chemical reactivity model, which separates energy into different contributions, allowing a detailed analysis of the energy distribution, such as the Activation Strain model (ASM),[3] the Energy Decomposition Analysis (EDA),[4] or the Reaction Force Analysis.[5] The latter model, proposed by Toro-Labbé, has been of much interest because it divides any elementary chemical step into different stages. Each stage represents a series of specific structural and electronic changes in the system. So, the reaction force analysis provides a framework to analyze the reaction mechanism through structural and electronic changes along with a reaction path.[6-11]

At the theoretical and computational level, the analysis of properties and decomposition of a reaction progress along a reaction path involves a series of general steps. It is mandatory to identify the minimum reaction path that connects the transition state with the reactant and product of the chemical reaction. This identification is usually performed by computing the intrinsic reaction coordinate (IRC).[12-13] Along the IRC, the evolution of any global or local molecular property can be followed up. In this way, distances between atoms, atomic charges, orbital energies, bond orders, etc., can be plotted and help us to understand the evolution of a chemical reaction. Of course, all this information must be processed and analyzed. Spreadsheets can be used to handle the data, but the extraction must be carried out manually so, in the process, the information can be altered or modified by human error.

Herein we show a new module, *Reaction Force*, implemented in *Eyringpy*,[14] to carry out the energy decomposition based on the reaction force model. On the top, structural and electronic changes along the reaction coordinate can be monitored. An interpolator has been coded and implemented to smooth the potential energy and reaction force curves. One of the advantages of this module is time, a complete analysis of the reaction mechanism takes place in seconds.

This work is divided into four Chapters. First, the concepts and reaction force theory used in the development of this module are presented. Details of the module's implementation, written in *Python 3.0.24*, are described in Chapter 2, emphasizing its internal structure (subroutines) and the type of calculations that can be executed. In Chapter 3, a series of pericyclic reactions reported in the literature were analyzed to validate the program. In Appendixes, there is a detailed user manual, starting with the installation and requirements needed before running any calculation (input files). Finally, the Conclusions and Perspectives of this work are discussed.

CHAPTER 1

BACKGROUND

"Every chemical reaction has a transition state."

-Derek Barton[15]

Chemical kinetics is one of the oldest branches of physical chemistry. Its study is intrinsically related to determining the rate of a reaction and its dependence on parameters such as concentration, temperature, catalysts, etc., and thus to understand all the steps involved in the reaction.[2, 16] For example, let us consider the 1,3 intramolecular hydrogen transfer

$$\boldsymbol{HSNO \rightleftharpoons SNOH},$$

where the hydrogen atom is transferred from sulfur (donor atom) to oxygen (acceptor atom). This reaction occurs in a single step and it can be characterized by the analysis of their energy profile along the process, which gives us information about the kinetics and the thermodynamic properties of the reaction. A more in-depth analysis of the reaction mechanism can be performed if a simultaneous exploration of the structural and electronic properties is done. Thus, to study how its energy and other properties change during the process is compulsory to understand this reaction mechanism.

1.1. Reaction mechanisms

Some chemical reactions occur in a single stage, but most of them happen in several elementary steps. Combining these steps of the reaction determines how the disappearance of the reactant(s) and the formation of product(s) is perceived. A reaction mechanism refers to a molecular description of how reactants are converted into products during a chemical reaction. It states the sequence of one or more elementary steps that define the route between

reactants and products. Elementary reactions take place in a single step.[17] A standard method for classifying elementary reactions uses the number of reactants taking part in the reaction; this is the molecularity. Elementary reactions are thus classified as unimolecular, bimolecular, or termolecular. Higher molecularities are unknown.[18]

- Unimolecular reactions. A reactant isomerizes or decomposes to give a product or products.[19] Reactions such as *cis-trans* isomerization, thermal decomposition, ring-opening, and racemization are usually unimolecular.[16]

$$\boldsymbol{A \rightarrow product(s)} \tag{1.1}$$

- Bimolecular reactions. Any elementary step that involves two reactants.[20]

$$\boldsymbol{A + B \rightarrow product(s)} \tag{1.2}$$

- Termolecular reactions. An elementary step that involves the simultaneous interaction among three reactants is called a termolecular reaction. The probability of a three-body collision is usually quite small and only a few such reactions are known.[16]

$$\boldsymbol{A + B + C \rightarrow product(s)} \tag{1.3}$$

Most reactions happen in more than one stage. Complex reactions proceed in several elementary chemical steps and invariably involve intermediates, which have a wide range of lifetimes.[21] Complex reaction mechanisms can conveniently be classified as consecutive, parallel, and reversible reactions.[22]

- Consecutive reactions. Reactants are converted into products through one or more intermediate steps. They are characterized by the product of the first reaction being a reactant in a subsequent process, and so on, leading to the formation of a final product.

$$\boldsymbol{A \longrightarrow B \longrightarrow C} \tag{1.4}$$

- Parallel reactions. Those reactions in which the same species participate in two or more competitive steps.[22-23]

$$\begin{aligned} \boldsymbol{A} &\longrightarrow \boldsymbol{B} \\ \boldsymbol{A} &\longrightarrow \boldsymbol{C} \end{aligned} \tag{1.5}$$

- Reversible reactions. The products of the initial reaction can recombine to regenerate the reactant.[22] The simplest reversible reactions are of the type:

$$\boldsymbol{A} \rightleftharpoons \boldsymbol{B} \tag{1.6}$$

1.2. Energy profiles and the transition state

Chemical reactions do not instantaneously come about; they require a finite time to get completed. This resistance to change implies that at the molecular level, individual steps in a mechanism need energy to take place. For a given step, the energy requirement will depend on the species involved in the reaction. A convenient way to discuss a chemical reaction is in terms of some energy profile, which covers aspects of mechanism, structure, and energy.[24-25]

The potential energy surface (PES) of a set of reactants is the potential energy as a function of their coordinates representing the molecular geometries of the system.[26] PES has $\boldsymbol{3N-5}$ (for two atoms) and $\boldsymbol{3N-6}$ (for three or more atoms) coordinate dimensions, where *N* is the number of atoms. A complete PES provides information about all possible chemical structures and all isomerization pathways interconnecting a given collection of atoms.[27]

The PES of a polyatomic molecule is difficult to visualize since it involves many dimensions. It is usual to take slices of the PES that involve just one coordinate. Thus, in the case of a single visualized dimension, the curve attempts to illustrate the minimum energy path (MEP) associated with varying the visualized coordinate.[27] The MEP is identified as the orthogonal trajectory that connects two local minima (the reactants and the products) via a common saddle point.[24] In elementary reactions, the existence of a transition state (TS) is usually assumed, which is the state of most positive energy between the reactants and the products through which an arrangement of atoms must pass on going from reactants to

products in either direction.[26] Some MEP examples are given in Figure 1.1, where the vertical axis is the potential energy, and the horizontal axis is the reaction coordinate.

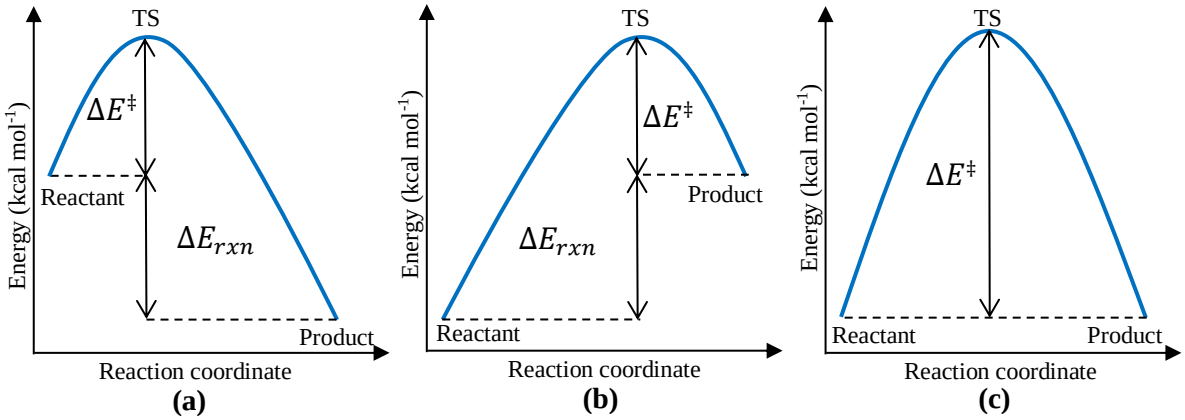

Figure 1.1. Energy profiles along the reaction coordinate for **(a)** exothermic, **(b)** endothermic, and **(c)** symmetrical reactions. TS is the transition state for each reaction, $\Delta \boldsymbol{E}^{\ddagger}$ is the activation barrier for the forward process, and $\Delta \boldsymbol{E_{rxn}}$ is the reaction energy.

When reactants (or products for the reverse process) have collided with enough energy of activation ($\Delta \boldsymbol{E}^{\ddagger}$) and with the proper orientation, they pass through the TS. All process need a determinate energy value to convert reactants into products, this is the reaction energy ($\Delta \boldsymbol{E_{rxn}}$), and it is equal to the energy difference between the products and the reactants.[18]

Let us consider a reaction between an atom A and a diatomic molecule BC, such as

$$\boldsymbol{A + BC \rightarrow AB + C},$$

To make the reaction happen, atom A must get closer to the molecule BC. While A gets closer to BC, the energy increases. This increase continues until the configuration A···B···C is formed, which is the transition state of the reaction, and later, products are obtained. When atom C separates to give molecule AB (or if the reaction merely reverses, to the original), the energy decreases again.[19]

The change in the energy when the transition state is reached from the initial state is called the activation energy for the forward process, $\Delta \boldsymbol{E^{\ddagger}_{for}}$. Similarly, the activation energy for the reverse process is $\Delta \boldsymbol{E^{\ddagger}_{rev}}$,

$$\boldsymbol{AB + C \rightarrow A + BC},$$

if $\Delta E^{\ddagger}_{for} < \Delta E^{\ddagger}_{rev}$, the reaction is exothermic (Figure 1.1a). If $\Delta E^{\ddagger}_{for} > \Delta E^{\ddagger}_{rev}$, the reaction is endothermic (Figure 1.1b). However, if both, $\Delta E^{\ddagger}_{for}$ and $\Delta E^{\ddagger}_{rev}$ are equal, it is told that the reaction has symmetrical activation barriers for both processes, forward and reverse, and $\Delta E_{rxn} = \mathbf{0}$ (Figure 1.1c).[21]

In multistep reactions, each step has its transition state.[18] These reactions are characterized by the appearance of an intermediate, which are a local potential energy minimum that is formed (directly or indirectly) from the reactants and reacts further to give the products of a chemical reaction.[26] An example of a complex reaction energy profile is given in Figure 1.2.

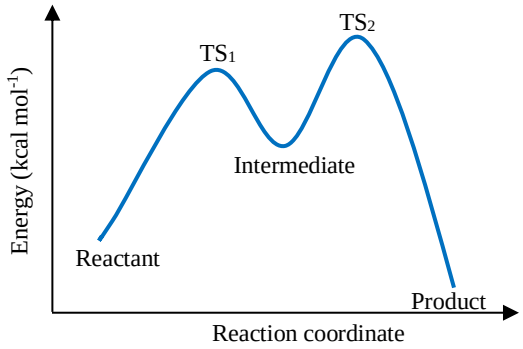

Figure 1.2. Energy profiles along with the reaction coordinate for a two steps mechanism. TS_1 and TS_2 represent the transition states for each step in the process.

1.3. Intrinsic Reaction Coordinate

Reaction path (RP) can be defined as the curve on the PES connecting reactants and products through the transition state.[28] This curve can be found by following the MEP from the transition state toward reactants and products. The MEP is composed of the two steepest descent reaction paths (SDRPs) that emerge from a saddle point in both directions (forward and reverse) along the principal axis of negative curvature and enter the two adjacent energy minima, each along the principal axis of least curvature.[24]

When we talk about the SDRP in mass-weighted Cartesian coordinates[28] that connects the TS to reactants and products on the PES, we refer to the Intrinsic Reaction Coordinate (IRC), which was introduced by Fukui in 1971.[12-13] This RP is a solution of the classical equations of motion, under the constraint that the velocity at any given point along

the path is zero. This produces the shortest path that connects reactants and products via a transition state.

The IRC can be viewed as generating a series of Cartesian coordinates by starting at the TS and following the SDRP down to the reactant and product minima, that is the solution of the following differential equation,

$$\frac{\boldsymbol{dx(s)}}{\boldsymbol{ds}} = -\frac{\boldsymbol{g(x)}}{|\boldsymbol{g(x)}|}, \tag{1.7}$$

where $\boldsymbol{x}$ is the path in mass-weighted Cartesian coordinate, $\boldsymbol{g}$ is the energy gradient of the PES, $|\boldsymbol{g}|$ is the norm of the vector $\boldsymbol{g}$, and $\boldsymbol{s}$ is the arc length along the path. The right side of equation corresponds to the normal coordinate eigenvector $\boldsymbol{v}$ with a negative value at the TS ($\boldsymbol{s} = \boldsymbol{0}$). For $\boldsymbol{s} > \boldsymbol{0}$, $\boldsymbol{v} = -\frac{\boldsymbol{g(x)}}{|\boldsymbol{g(x)}|}$, and $\boldsymbol{v} = \frac{\boldsymbol{g(x)}}{|\boldsymbol{g(x)}|}$ for $\boldsymbol{s} < \boldsymbol{0}$.[12, 29]

Since IRC is defined by an ordinary differential equation (ODE), numerical integration techniques can be used. Solving Equation 1.7. needs special care, and several specialized methods have been developed and reviewed in the literature.[30-31] Numerical methods for integrating ODEs are classified as explicit or implicit. Explicit methods only use the information at the current point to define the next position. In contrast, implicit methods use additional information from the next point (typically derivative information), which means that they include some sort iterative algorithm to converge at the endpoint of each step. Therefore, implicit methods are most costly, but they allow larger step sizes, while explicit methods are limited to a rather small step size.[30-33]

The main idea to solve IRC is shown in Figure 1.3. It involves walking down the IRC in several steps with fixed step size n, each of them constructed starting from an initial point (P_i) on the path (shown in blue) construct auxiliary point (P') located n/2 away from P_i along tangent (shown in orange). On a hypersphere of radius n/2 centered at P' search for the point of lowest energy (P_f). This latter point is the new point on the IRC path. This constrained search needs several energy and gradient calculations. This sequence is repeated until the geometry convergence criteria are fulfilled in a direction along the pathway.[34]

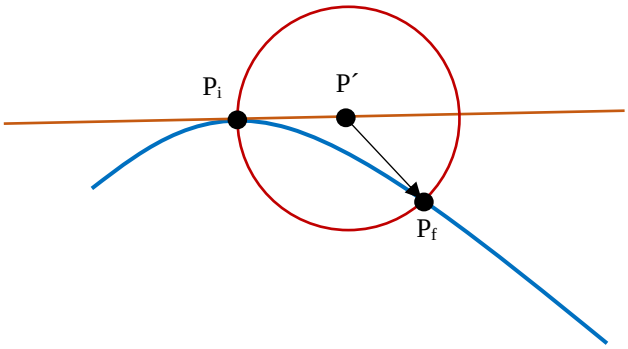

Figure 1.3. IRC method. P_i is an initial point of the IRC path, P' is the constructed auxiliary point and P_f is the new point on the IRC path.

1.4. The reaction force analysis

In 1999, Toro-Labbé introduced the concept of reaction force **F**(ξ).[5] This has proved to be a suitable tool for studying reaction mechanisms and identifying characteristic processes taking place in chemical reactions. The evolution of structural and electronic changes along the reaction coordinate produces valuable information about reaction mechanisms. Several processes in terms of the reaction force have been analyzed, including intramolecular and intermolecular proton transfers,[35-46] conformational changes,[47-48] bond-dissociation, and bond-formation,[49-50] S_N2 substitution,[51-52] and solvent effects.[53-54]

Based on the classical expression for a force, the reaction force is defined as the negative gradient of potential energy. For a chemical or physical process,

$$\boldsymbol{F}(\boldsymbol{\xi}) = -\frac{\boldsymbol{\partial V}(\boldsymbol{\xi})}{\boldsymbol{\partial \xi}}, \tag{1.8}$$

where V(ξ) is the profile of the potential energy of the total system along some well-defined path ξ (IRC) from reactants to products.[5-11] Although a chemical reaction occurs through the simultaneous change of different geometrical parameters in a multidimensional space, this multidimensional motion is condensed in the reaction coordinate ξ, thus **F**(ξ) is a global property of the reaction that has all the information concerning the specific interactions that drive the reaction from reactants to products.[36] It provides the elements to characterize the different reaction mechanisms that might be operating along with the reaction coordinate,[40]

and its profile is dictated by that of potential energy V(ξ), but reaction force F(ξ) can be expected to have more features, has a zero at every maximum or minimum of V(ξ),

$$\left(\frac{\partial \boldsymbol{V}(\boldsymbol{\xi})}{\partial \boldsymbol{\xi}}\right)_{\boldsymbol{V_{max}},\boldsymbol{V_{min}}} = \mathbf{0} = \boldsymbol{F}(\boldsymbol{V_{max}}, \boldsymbol{V_{min}}) \tag{1.9}$$

and has a maximum and minimum at each inflexion point of V (ξ),

$$\left(\frac{\partial \boldsymbol{F}(\boldsymbol{\xi})}{\partial \boldsymbol{\xi}}\right)_{\boldsymbol{V_{infl}}} = -\left(\frac{\partial^2 \boldsymbol{V}(\boldsymbol{\xi})}{\partial \boldsymbol{\xi}^2}\right)_{\boldsymbol{V_{infl}}} = \mathbf{0} \tag{1.10}$$

Another exciting aspect of reaction force analysis is the reaction force constant, κ(ξ), introduced by Jaque and co-workers.[55] It is defined as the second derivative of a potential energy along with the IRC, ξ, from reactants to products,

$$k(\xi) = \frac{\partial^2 V(\boldsymbol{\xi})}{\partial \boldsymbol{\xi}^2} = -\frac{\partial \boldsymbol{F}(\boldsymbol{\xi})}{\partial \boldsymbol{\xi}} \tag{1.18}$$

This has been employed to analyze projected force constants along IRC,[55] and as an indicator of synchronicity or nonsynchronicity in some mechanisms, such as double proton transfer reactions,[56] and cycloaddition processes.[57]

The zero, minima, and maxima of F(ξ) represent three key points along with the IRC. Figure 1.4 shows how these points divide V(ξ), F(ξ), and κ(ξ) profiles into four zones. These four zones define three regions along with the IRC, where specific interactions that might be driving the reaction are turned on and off during the process. It has been demonstrated that analyzing a process in terms of these regions provides significant insight into its mechanism and the roles of external factors.[35-54] These studies have shown that, in general, each of the regions defined by **F**(ξ) is characterized by some specific changes in the reaction.

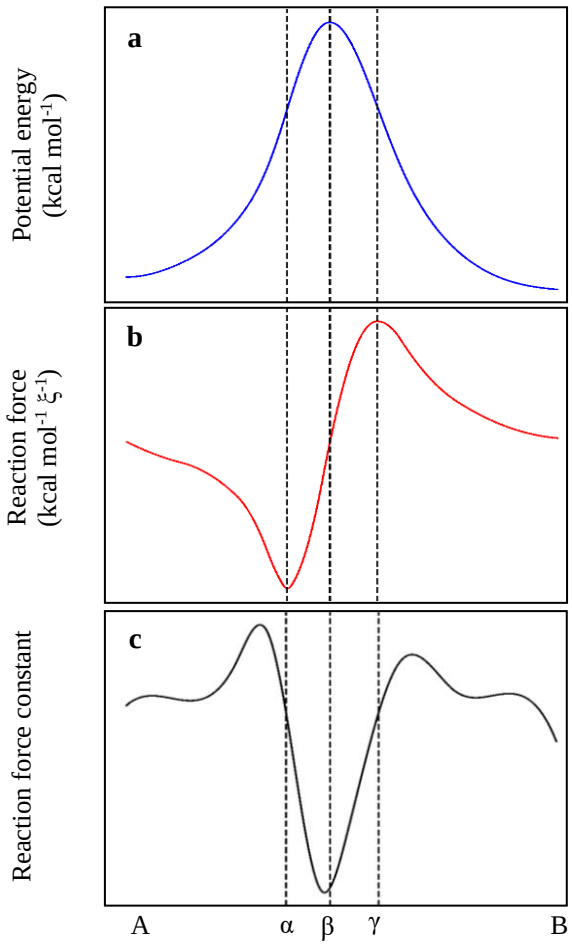

Figure 1.4. (a) Potential energy, (b) reaction force, and (c) reaction force constant profiles along with the IRC for a reaction, A↔B. The points α, β, γ correspond to the minimum, zero and maximum of the force, the vertical lines divide the reaction into four zones.

Figure 1.4b shows a typical F(ξ) profile and its divisions. The first region corresponds to zone 1 ($A \rightarrow \alpha$), 'reactants' region and it involves preparation and structural distortions of the reactants. At the force minimum, $\xi = \alpha$, the system is described as an activated state of the reactants. The second region, which corresponds to zone 2 ($\alpha \rightarrow \beta$) and zone 3 ($\beta \rightarrow \gamma$), is called 'transition to product' region and it is characterized by bond breaking/formation and significant electronic reordering. At the force maximum, $\xi = \gamma$, the system reaches what may be viewed as an activated or distorted state of the products. In the final region, zone 4 ($\gamma \rightarrow B$), called 'products' region, the system relaxes structurally to their equilibrium form in the products.[7-11]

The energy changes along the reaction progress can be expressed in terms of F(ξ), using Equation 1.8 for each of the four zones, energy changes may be expressed as

$$\Delta \boldsymbol{E_1} = -\int_{\xi=A}^{\xi=\alpha} \boldsymbol{F}(\boldsymbol{\xi})\, \boldsymbol{d\xi}, \tag{1.11}$$

$$\Delta \boldsymbol{E_2} = -\int_{\xi=\alpha}^{\xi=\beta} \boldsymbol{F}(\boldsymbol{\xi})\, \boldsymbol{d\xi}, \tag{1.12}$$

$$\Delta \boldsymbol{E_3} = -\int_{\xi=\beta}^{\xi=\gamma} \boldsymbol{F}(\boldsymbol{\xi})\, \boldsymbol{d\xi}, \tag{1.13}$$

$$\Delta \boldsymbol{E_4} = -\int_{\xi=\gamma}^{\xi=B} \boldsymbol{F}(\boldsymbol{\xi}) * \boldsymbol{d\xi}, \tag{1.14}$$

where $\Delta \boldsymbol{E_{f,i}}$ are the energy changes in the i^{th} zones of the forward process. Forward and reverse activation barriers, and the total reaction energy can also be expressed in terms of **F**(ξ), as the sum of energy changes,[6-11]

$$\Delta \boldsymbol{E}_{for}^{\ddagger} = \Delta \boldsymbol{E_1} + \Delta \boldsymbol{E_2} = -\int_{\xi=A}^{\xi=\beta} \boldsymbol{F}(\boldsymbol{\xi}) * \boldsymbol{d\xi} \tag{1.15}$$

$$\Delta \boldsymbol{E}_{rev}^{\ddagger} = -\Delta \boldsymbol{E_3} - \Delta \boldsymbol{E_4} = \int_{\xi=\beta}^{\xi=B} \boldsymbol{F}(\boldsymbol{\xi}) * \boldsymbol{d\xi} \tag{1.16}$$

$$\Delta \boldsymbol{E_{rxn}} = -\int_{\xi=A}^{\xi=B} \boldsymbol{F}(\boldsymbol{\xi}) * \boldsymbol{d\xi} = \Delta \boldsymbol{E}_{for}^{\ddagger} - \Delta \boldsymbol{E}_{rev}^{\ddagger} \tag{1.17}$$

We saw in Section 1.1.3 that a reaction might also proceed through one or more intermediates. Reaction force analysis can take place for each step of the process. The corresponding **F**(ξ), and κ(ξ), are again obtained employing Equations 1.8 and 1.18, and they are simply extensions of those in Figure 1.4b and 1.4c, with no new features. All reaction force minima and maxima again define stages of the process, which are either dominated by structural changes or involve transitions to new species.[8]

CHAPTER 2

PROGRAM DESCRIPTION

"In some ways, programming is like painting. You start with a blank canvas and certain basic raw materials. You use a combination of science, art, and craft to determine what to do with them."

-Andrew Hunt

Eyringpy[14] is a modular program for calculating thermochemical properties and rate constants for reactions in the gas phase and solution. Thermochemical properties are estimated through the canonical ensemble and rate constants are computed according to the transition state theory. To complement this kinetic analysis, a new module has been implemented in *Eyringpy*, called *Reaction Force*, which uses the theory proposed by Toro-Labbé to perform a complete reaction mechanism analysis. Unimolecular, bimolecular, and termolecular reactions are supported. Potential energy decomposition is performed following Reaction Force theory, dividing energy contributions into the three proposed stages, taking data from IRC calculations. It may interpolate potential energy, reaction force, and reaction force constant profiles to get smoother curves. Properties analysis along with the IRC may be performed taking data from IRC. Available properties to be analyzed are bond lengths, Wiberg bond indices, dipole moments, HOMO-LUMO gap, and natural charges. One advantage of this module is that it has been programmed in subroutines, which allows us to add new properties easily. Also, a plotter option has been implemented to visualize how properties change along with the IRC.

Reaction force is written in *Python 3.0*[58] and it is divided into 21 subroutines. It has a user-friendly interface and a simple input format. The module's flowchart is shown in Figure 2.1 and the user manual is in Appendix C.

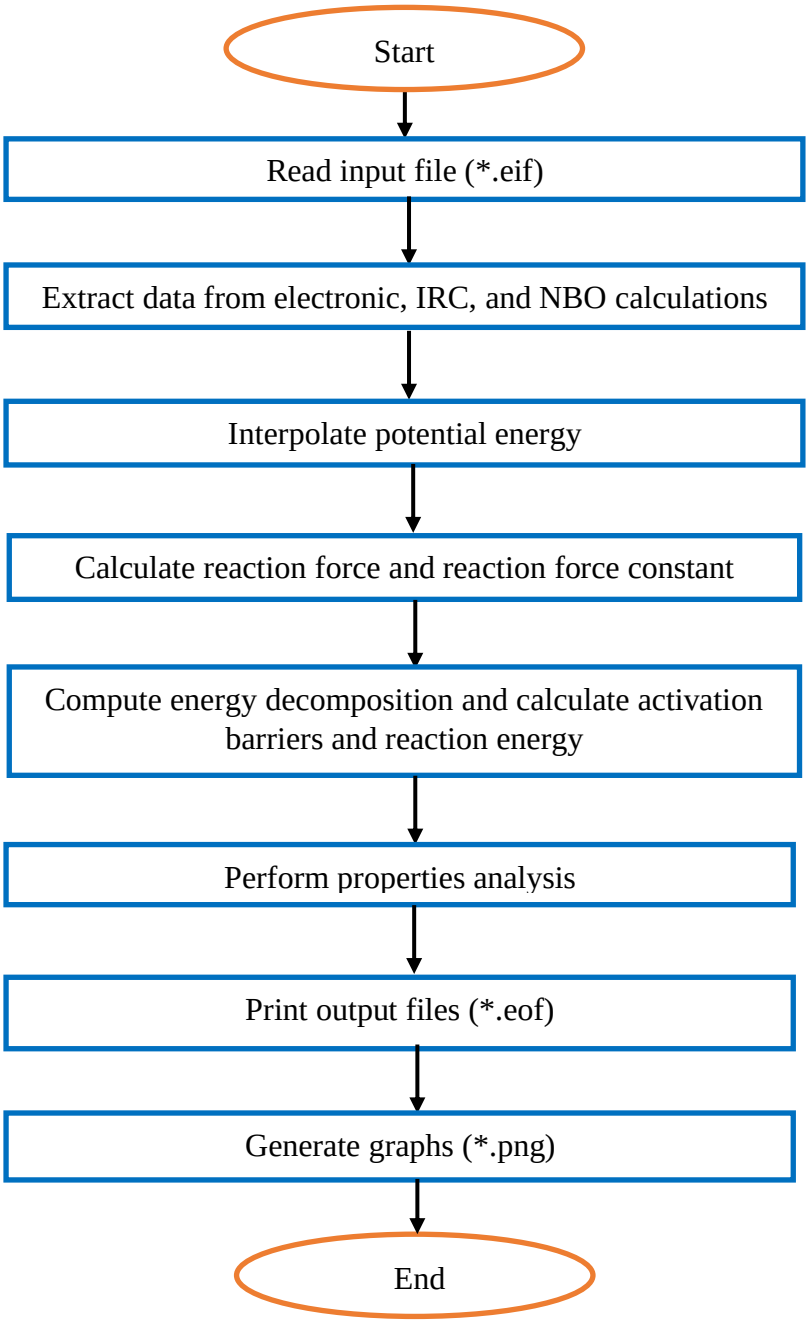

Figure 2.1 *Reaction Force* flowchart.

2.1 Subroutines

2.1.1 Inputwriter

Inputwriter creates a sample of the input file (*.eif). This file contains the keywords to execute the program.

2.1.2. Inputreader

This subroutine reads the input file and extracts information to determine the interpolation method and its input parameters, the names of the output files (reactants, products, and transition state) and those of the IRC output files (forward and reverse) to perform reaction force analysis (energy decomposition) and properties analysis.

Keywords of the input file are described below. Some of them have default values, which will be used if the user skips them in the input file (this allows us to have concise input files). Those options that are not in default should always be specified. Lines that start with # are comments and the reader ignores them.

a) The following keywords correspond to the name of the *Gaussian* frequency and IRC calculations. These files must be in the same folder as the input file (*.eif).

- REACTn. It is a variable of type character with the name of the *Gaussian* frequency output files that correspond to the *n* reactants. It may be absent if a comparison between the expected and interpolated energy values is not necessary. For instance, depending on the reaction, whether unimolecular, bimolecular, or termolecular, *n* takes the values 1, 2, or 3. It has no default value.

  Format: `REACT1 reactfilename1.out`
  `REACT2 reactfilename2.out`

- TS. It is a variable of type character with the name of the *Gaussian* frequency output file that corresponds to the transition state. It may be absent if a comparison between expected and interpolated energy values is not necessary. It has no default value.

  Format: TS tsfilename.out

- PRODn. It is a variable of type character with the name of the *Gaussian* frequency

output files that correspond to the *n* products. It may be absent if a comparison between expected and interpolated energy values is not necessary. For instance, depending on the reaction, whether unimolecular, bimolecular, or termolecular, *n* takes the values 1, 2, or 3. It has no default value.

Format: `PROD1 productfilename1.out`
`PROD2 productfilename2.out`

- IRC. It is a variable of type character with the name of the *Gaussian* IRC output files that correspond to the transition state provided by the user in the TS keyword. The names of the output files correspond to the forward and reverse IRC calculations. It is possible to provide one or two *Gaussian* IRC output files, but at less one must be provided. It has no default value.

  Format: `IRC forwardfilename.out  reversefilename.out`

b) All the following keywords correspond to the interpolation method.

- INTERP. It is the interpolation method and only one value in this version is possible SPLINE. Future versions will include other interpolation methods. It has no default value.

  Format: `INTERP SPLINE`

- ORDER. It is only used for interpolation and denotes the interpolation order. It takes integer values between 3 and 5. Its default value is 3.

  Format: `ORDER 5`

- SMOOTH. It is only used for interpolation and denotes the smooth interpolation factor. It takes positive integer or decimal values. Its default value is 0.0.

  Format: `SMOOTH 1E-8`

- NPOINTS. It is only used for interpolation and denotes the number of new points to generate. It takes only positive and integer values. Its default value is 0.

Format: `NPOINTS 1000`

- DISCRIM. This keyword is optional. It is used when the user needs to remove those points which go off the original potential energy curve by comparing it with the interpolated one. It denotes two parameters: the threshold value to discriminate points of the potential energy curve and the units of the threshold value. The threshold value must be a positive integer or decimal number and the threshold unit could be KCAL (kilocalories) or HA (Hartrees). This keyword is only activated if the INTERP keyword is activated too. Threshold value always must be specified, it has not a default value. If the threshold unit is not specified, it takes KCAL value.
  Format: `DISCRIM 0.05 HA`

c) All the following keywords correspond to the property analysis through the IRC profile. These are divided into three groups, depending on the number of atoms specified to perform the property analysis: no atoms, one atom, and two atoms.

- HOMOLUMO. It is a variable of type character. This keyword must be present if a bandgap analysis is required. It takes TRUE or FALSE value. It has no default value.
  Format: `HOMOLUMO TRUE`

- DIPOLE. It is a variable of type character. This keyword must be present if a dipole moment analysis is required. It takes TRUE or FALSE value. It has no default value.
  Format: `DIPOLE TRUE`

- NATCHARGE. This keyword must be present if a charge analysis is required. It denotes the atoms to analyze the charge change. It can take more than one value if the analysis is required for more than one atom. It takes values from 1 to the maximum number of atoms present in the system. It has no default value.
  Format: `CHARGE 1 2 3 4`

- BONDLEN. This keyword must be present if a bond length analysis is required. It

denotes the pair of atoms to analyze the bond length changes. The atom numbers for the bond length must be separated by a hyphen (-). If more than one bond length is required to analyze, BONDLEN can take more than one pair of values and a blank space must separate each pair. The atom numbers take values from 1 to the maximum number of atoms present in the system. It has no default value.

Format: `BONDLEN 1-2 3-4 1-4`

- WIBERG. This keyword must be present if a Wiberg analysis is required. It denotes the pair of atoms to analyze the Wiberg bond indices changes. Atom numbers for the bond length must be separated by a hyphen (-). If more than one bond length is required to analyze, WIBERG can take more than one pair of values and a blank space must separate each pair. The atom numbers take values from 1 to the maximum number of atoms present in the system. It has no default value.

  Format: `WIBERG 1-2 3-4 1-4`

d) Outputs: All the following keywords are related to output files generated by the module.

- NBO. It is a variable of type character. This keyword must be present if *Gaussian* input files for Natural Bond Orbital (NBO) calculations must be generated. An input file (.inp) with *Gaussian*[59] NBO specifications is generated for each structure of the intrinsic reaction coordinate. This keyword requires four default values, in the following order, which are: memory size, functional, basis, and NBO version. More parameters could be given if the user requires some other route specifications, such as scf=tight. It has no default values. At least, the first four parameters must be specified.

  Format: `NBO 10 TPSSTPSS def2TZVP NBO6`

- XYZ. It is a variable of type character. This keyword must be present if an XYZ file with all the molecule geometries of the IRC must be generated. It takes TRUE or FALSE value. It has no default value.

  Format: `XYZ TRUE`

- GRAPH. It is a variable of type character. This keyword must be present if graphics must be generated. It takes the names of the keywords related to the properties to be analyzed as a graph. It has no default value.

  Format: `GRAPH IRC HOMOLUMO BONDLEN`

2.1.3. Constants

The Constants subroutine is a library that contains constants values in Table B1 and unit conversions in Table B2 (Appendix B) of the program. The numerical values of the constants have been taken from the database of the National Institute of Standards and Technology (NIST).[60]

2.1.4. Gaussparser

The Gaussparser subroutine contains the functions that extract data from *Gaussian* electronic structure calculations of each stationary state (reactant(s), product(s), and transition state).

2.1.5. IRCparser

The IRCparser subroutine contains the functions that extract the reaction coordinates and potential energies from *Gaussian* IRC calculations (forward and reverse) of the transition state provided by the user.

2.1.6. Coordinatesparser

The Coordinatesparser subroutine contains the functions that extract the atoms' coordinates (x, y, z) of each molecule geometry along with the IRC from *Gaussian* IRC calculations.

2.1.7. Thermochemistry

This subroutine determines the activation and reaction energies at 0 K, with the electronic energy taken from the Gaussian electronic structure calculations.

2.1.8. Interpolation

The Interpolation subroutine uses the spline method to interpolate the potential energy from the IRCdata library to smooth potential energy curves. The *scipy.interpolate.UnivariateSpline* function from SciPy[61] library was used.

2.1.9. Reactionforce

The Reactionforce subroutine calculates and interpolates the reaction force as the negative derivative of the potential energy with respect to the IRC, Equation 1.9. The *scipy.interpolate.UnivariateSpline.derivative* function from SciPy[61] library was used.

2.1.10. Forceconstant

The Forceconstant subroutine calculates and interpolates the reaction force constant as the second derivative of the potential energy with respect to the IRC, Equation 1.19. The *scipy.interpolate.UnivariateSpline.derivative* function from SciPy[61] library was used.

2.1.11. Energies

The Energies subroutine computes energy decomposition into the four zones proposed in Reaction Force theory using Equations 1.12 - 15. Then, it calculates activation barriers (forward and reverse) using Equations 1.16 - 17, and reaction energy using Equation 1.18. The *scipy.interpolate.UnivariateSpline.integral* function from SciPy[61] library was used.

2.1.12. Discriminate

The Discriminate subroutine allows removing those points that go off the curve. To remove them, a threshold value provided by the user in the input file is compared with the distance between the interpolated and original energy points. This subroutine uses the formula of distance between two points in *xy*-space,

$$\boldsymbol{d = \sqrt{(x_2 - x_1)^2 + (y_2 - y_1)^2}},\tag{2.1}$$

where $\boldsymbol{x_n}$ and $\boldsymbol{y_n}$ are the reaction coordinates and potential energies, respectively; $\boldsymbol{n = 1}$ correspond to the original points taken from IRC Gaussian files, and $\boldsymbol{n = 2}$ to the interpolated points. Those pairs of points that have distances higher than the threshold value are removed.

2.1.13. Bondlength

The Bondlength subroutine uses the formula of distance between two points in *xyz*-space to calculate the distances between two atoms,

$$\boldsymbol{d = \sqrt{(x_2 - x_1)^2 + (y_2 - y_1)^2 + (z_2 - z_1)^2}}\tag{2.2}$$

where $\boldsymbol{x_n, y_n, z_n}$ correspond to the atoms' coordinates taken from Coordinatesdata library for atom 1 ($\boldsymbol{n = 1}$) and atom 2 ($\boldsymbol{n = 2}$) specified by the user in the input file keyword.

2.1.14. Wiberg

The Wibergparser subroutine contains the functions that extract Wiberg bond indices from *Gaussian* NBO calculations for each structure of the IRC.

2.1.15. Naturalcharge

The Naturalchargeparser subroutine contains the functions that extract natural charges from *Gaussian* NBO calculations for all the atoms in each structure of the IRC.

2.1.16. Homolumo

The Homolumoparser subroutine contains the functions that extract Highest Occupied Molecular Orbital (HOMO) and Lowest Unoccupied Molecular Orbital (LUMO) from *Gaussian* NBO calculations for each structure of the IRC. It calculates bandgap energy as the difference between HOMO and LUMO energies.

2.1.17. Dipole

The Dipoleparser subroutine contains the functions that extract dipole moment from *Gaussian* outputs for each structure of the IRC.

2.1.18. Outputwriter

The Outputwriter subroutine writes the *Eyringpy* output files (.eof) with the results according to the specifications provided in the input file. For property analysis, it writes an output file for each property specified by the user.

2.1.19. XYZwriter

The XYZwriter creates an XYZ file (.xyz) with the molecule geometry of each point along with the IRC. This output file may be read by any computational chemistry program. The formatting of the .xyz file format is as follows:

```
<number of atoms>
comment line
<element> <X> <Y> <Z>
```

2.1.20. NBOwriter

The NBOwriter creates NBO *Gaussian* input files (.inp). An input file is generated for each molecule geometry of the IRC.

2.1.21. Plotter

The Plotter subroutine creates the graphs (.png) according to user specifications.

CHAPTER 3

PROGRAM VALIDATION

"May the force be with you".

-George Lucas

3.1. Introduction

Woodward and Hoffmann defined pericyclic reactions as concerted reactions in which all bonds are made or broken around a circle.[62-63] These reactions share the feature of having a cyclic TS with a concerted movement of electrons simultaneously breaking bonds and making bonds. Cycloadditions, electrocyclic reactions, sigmatropic rearrangements, and group transfer reactions are some examples of this type of reactions.[64-65]

Cycloaddition reactions are those in which two or more unsaturated molecules (or parts of the same molecule) combine with the formation of a cyclic adduct in which there is a net reduction of the bond order.[26] The typical cycloaddition reaction is the Diels-Alder (DA) reaction, discovered in the 1920s by Diels and Alder.[66] The most straightforward DA reaction is between *s*-*cis*-1,3-butadiene and ethylene to form cyclohexene (Figure 3.1.1).

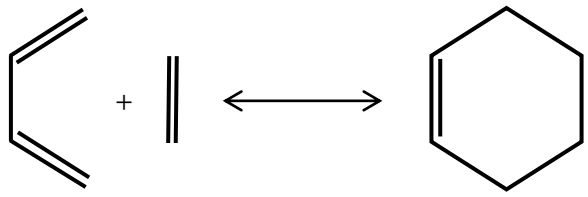

Figure 3.1.1. DA cycloaddition between *s*-cis-1,3-butadiene and ethylene

Electrocyclic reactions are unimolecular reactions.[67] They are characterized by the creation of a ring from an open-chain conjugated system, involving the formation of a σ-bond between the termini of a fully conjugated linear π-electron system (or a linear fragment of a π-electron system) and a decrease by one in the number of π-bonds, or the reverse of that

process.[26] One typical reaction of this class is the ring-closing of 1,3,5-hexatriene to 1,3-cyclohexadiene (Figure 3.1.2).

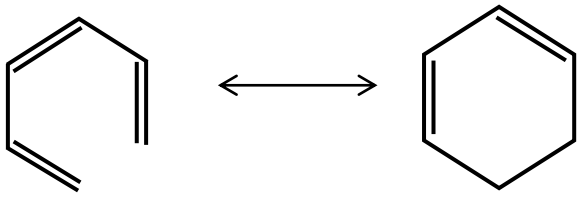

Figure 3.1.2. Electrocyclization of 1,3,5-hexatriene to 1,3-cyclohexadiene

Sigmatropic rearrangements involve both the creation of a new σ-bond between atoms previously not directly unlinked and the breaking of an existing σ-bond. There is a concurrent relocation of π-bonds in the molecule. Considering only atoms within the cyclic array undergoing reorganization, if the numbers of these in the two fragments are designated i and j, then the rearrangement is said to be a sigmatropic change of order [i, j].[26, 65] For instance, the degenerate [3,3] Cope rearrangement of 1,5-hexadiene (Figure 3.1.3).

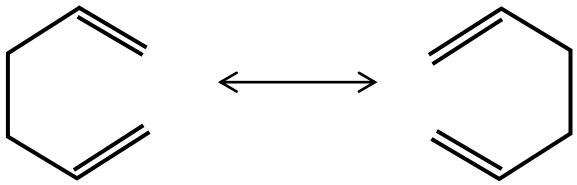

Figure 3.1.3. Degenerate [3,3] Cope rearrangement of 1,5-hexadiene

Double group transfer (DGT) reactions are chemical transformations that occur through the simultaneous migration of two atoms or groups from one compound to another in a concerted RP. The archetypical DGT reaction process is the thermally allowed concerted transfer of two hydrogen atoms from ethane to ethylene (Figure 3.1.4).[67]

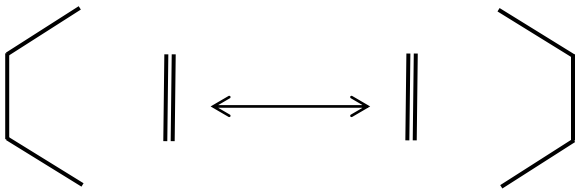

Figure 3.1.4. DGT from ethane to ethylene.

To validate the module, four pericyclic test systems have been chosen: the DA reaction between *s-cis*-1,3-butadiene and ethylene, the electrocyclization of 1,3,5-hexatriene to 1,3-cyclohexadiene, the degenerate [3,3] Cope rearrangement of 1,5-hexadiene and the DGT transfer between ethane and ethylene.[68]

3.2. Computational details

All the computations were carried out at the DFT (Density Functional Theory) level with the M11 functional and the 6-31+G(d,p) basis set, using the *Gaussian* 16 package[59]. It has been shown that hybrid-meta KS-DFT methods with a double zeta basis sets perform well for barrier heights and exothermicities in DA reactions, and those that incorporate a certain percentage of exact HF exchange and medium-range electron correlation perform in good order for TS geometry optimizations;[69] this is the reason why M11 functional, and 6-31+G(d,p) basis set were chosen.

The MEP in going from reactants to products was calculated through the IRC procedure in mass-weighted internal coordinates. Frequency computations on all stationary states (reactants, products, and transition state) were performed to confirm the nature of the corresponding critical point and to obtain electronic energies. TS structure shows only one imaginary frequency. Natural charges and Wiberg bond indices (WBI) were obtained using the NBO version 3.0 procedure in *Gaussian*.[70] Potential energies and reaction coordinates were taken from IRC calculations. Reaction force calculation, energy decomposition into the three reaction stages, structural and electronic analysis were computed using the *Reaction Force* module in *Eyringpy.* All transition state's coordinates are given in Appendix D.

3.3. Results and discussions

3.3.1. Diels-Alder reaction between *s-cis*-1,3-butadiene and ethylene

DA reaction of *s-cis*-butadiene and ethylene has been extensively investigated. Two possible pathways have been proposed in the literature: a concerted pathway and an alternative stepwise diradical mechanism. There is strong evidence than the concerted pathway is favored over the alternative stepwise by 2-7 kcal mol^{-1}.[68] So, herein just the concerted pathway has been selected. The M11/6-31+G(d,p) TS structure of this DA-

reaction is shown in Figure 3.3.1. At the TS, the C1-C3 and C2-C6 distances are both 2.277 Å, indicating a synchronous pathway, and they are close to values reported in the literature at the M06-2X/6-311++G(2d,p) level (2.248 Å).[71]

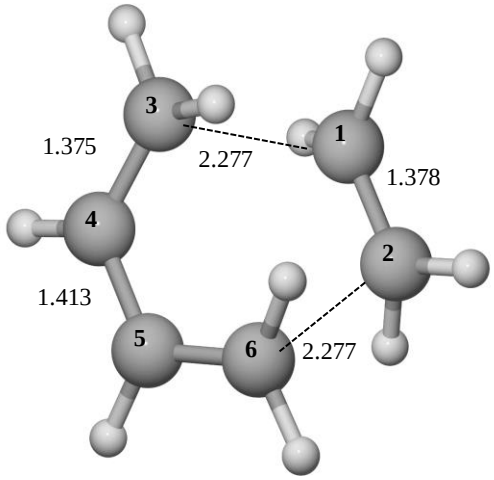

Figure 3.3.1. Transition state corresponding to DA reaction between *s-cis*-butadiene and ethylene (*cis*-TS). Bond lengths are shown in Angstroms.

Before the analysis, let us discuss a couple of particularities of this reaction. The typical experimental energy barrier reported for the DA reaction between *s-trans*-butadiene and ethylene is 27.5 kcal mol^{-1}.[71-72]. In our case, the relative free energy between *s-trans* and *s-cis*-butadiene is 1.8 kcal mol^{-1}, while the relative free energy between the *cis*-TS and *s-trans*-butadiene + ethylene fragments ($\Delta G^{\ddagger}$) is 34.1 kcal mol^{-1} computed at the M11 level (Table 3.3.1), which is comparable with the M06-2X value of 33.8 kcal mol^{-1}. This inconsistency in the barriers is not discussed in detail in the literature. The reason for such difference in the free energy barriers is because the experimental one is obtained in solution and our barrier is computed in the gas phase, so there are solvent effects that should be considered. For the reaction force analysis, this is not a big deal, but we should revisit it soon.

Table 3.3.1. The relative Gibbs free energies ΔG (kcal mol^{-1}) of selected stationary points in DA reaction using the M11/6-31+G(d,p) level.

	ΔG
s-trans-butadiene + ethylene	0.0
s-cis-butadiene + ethylene	1.8
cis-TS	34.1
hexene	-27.1

All values are reported in kcal mol^{-1}. The *cis*-TS structure corresponds to TS in Figure 3.3.1.

The *s-trans* conformation of butadiene has a lower energy than *s-cis* conformation as it shows in Table 3.3.1, but the butadiene cannot react in *s-trans* conformation as this introduces an impossibly strained trans double bond in the six-membered ring adduct (Figure 3.3.2). So, the DA reaction proceeds via a *s-cis* conformation which gives a stable *cis* double bond in the cycloadduct. Butadiene which exists in *s-trans* conformation must therefore take up the higher energy *s-cis* conformation to undergo the DA reaction with the ethylene (Figure 3.3.3).[73]

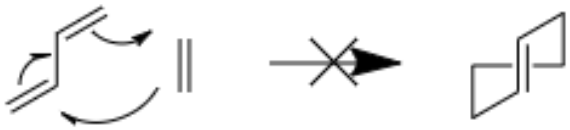

Figure 3.3.2. No DA reaction between *s-trans*-butadiene and ethylene.

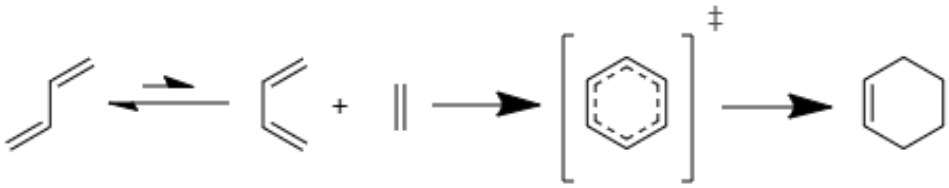

Figure 3.3.3. DA reaction between butadiene and ethylene.

Once the TS was captured, the next step was to confirm that it relates to the correct minima. On the side of the products, IRC leads us directly to hexadiene in a twisted chair conformation (see Figure 3.3.4). On the reactive side, IRC stops abruptly in the *cis*-isomer when the C1-C3 and C2-C6 distances are 3.243 Å! It means that, at least at the M11 level, the DA reaction involves two steps, first the butadiene isomerization (ΔG = 1.8 kcal mol^{-1}), and second the reaction between *s-cis*-butadiene and ethylene. At this point, DA reaction is a thermally allowed cycloaddition. If this reaction proceeds by two-steps, the cycloaddition of ethylene to *s-cis*-butadiene is the limiting step.

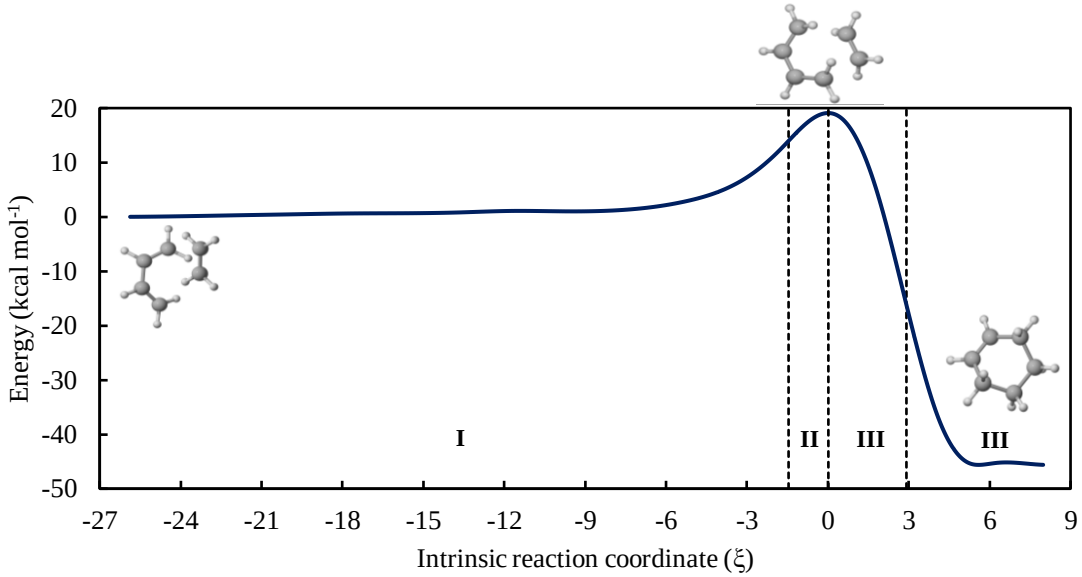

Figure 3.3.4. V(ξ) profile in kcal mol^{-1} of the DA reaction between *s-cis*-butadiene and ethylene. Reactants, TS, and product structures of the reaction at M11/6-31+G(d,p) level are shown. The dashed vertical lines delimit the reactant region (I), transition state region (II and III), and product region (IV).

Let us now to analyze the reaction force and the variation of some descriptors (as bond distances, WBI, and atomic charges) along the IRC to try to understand the DA reaction in detail, but most importantly for our purposes, to validate the *Reaction Force module* in *Eyringpy*. The F(ξ) profile, the evolution of the C-C distances, the corresponding WBI, and the atomic changes for the concerted DA reaction mechanism of *s-cis*-butadiene and ethylene are depicted in Figure 3.3.5.

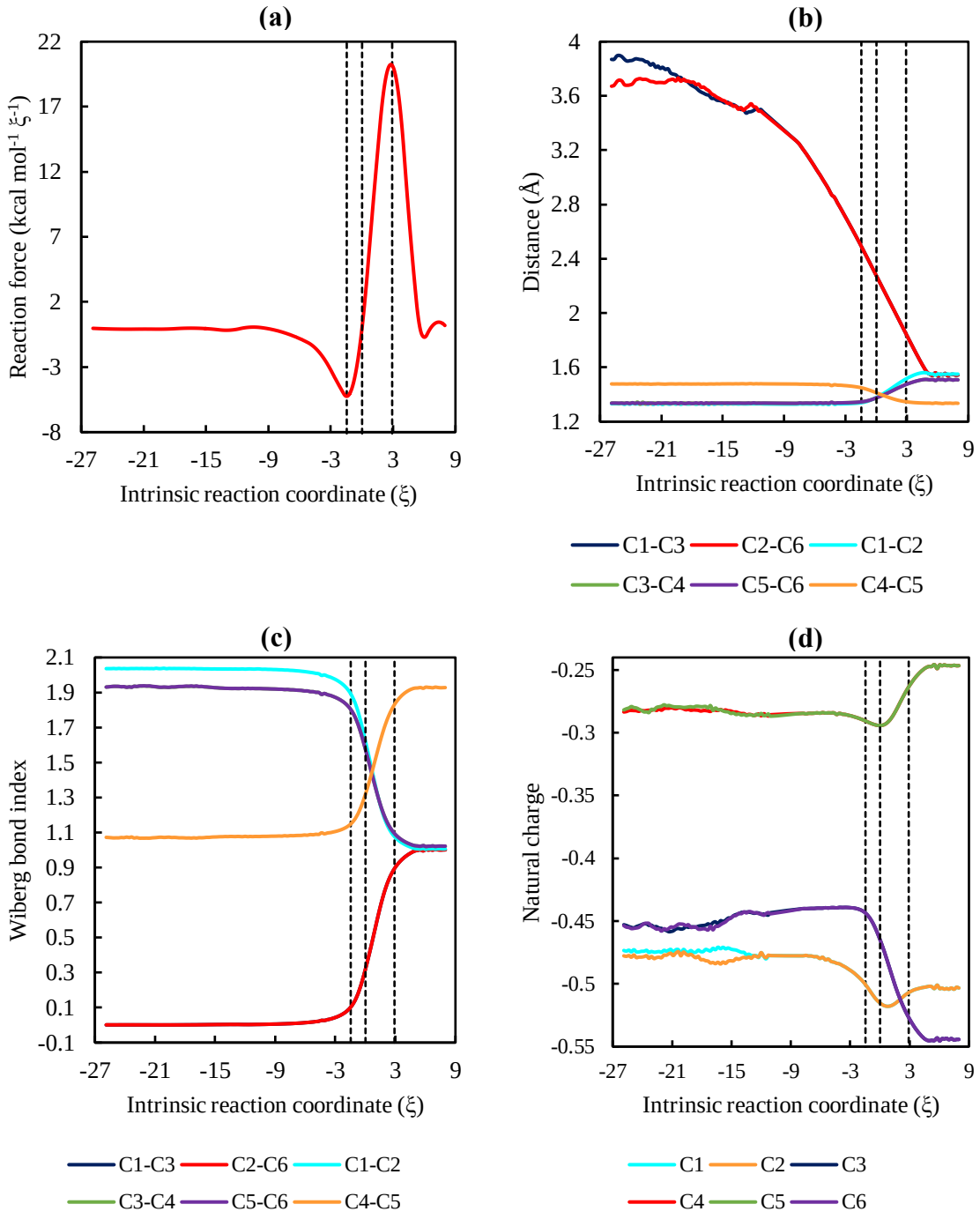

Figure 3.3.5. (a) F(ξ) in kcal mol^{-1} ξ^{-1}, **(b)**, evolution of all relevant bonds, **(c)** Wiberg bond indices, and **(d)** natural charges profiles of the carbon atoms of the DA reaction between *s-cis*-butadiene and ethylene. The dashed vertical lines delimit the different regions. From left to right, the delimited zones are reactant region (I), transition state region (II and III), and product region (IV).

The natural division provided by the reaction force analysis is discussed in detail in Chapter 1. In our case, ξ = -1.46 and ξ = 2.91 delimit the transition state region. Briefly, the energetics recovered by the integration of the reaction force profile is reported in Table 3.3.2. Note that the reaction energy (ΔE_{rxn}) computed by the integration of the reaction force (-45.6 kcal mol^{-1}) is just 0.2 kcal mol^{-1} lower than ΔE calculated as the difference of the energies between reactants and products, validating our results.

Table 3.3.2. Energy quantities associated with the DA reaction between *s-cis*-butadiene and ethylene computed at the M11/6-31+G(d,p) level.

$\boldsymbol{W_1}$	$\boldsymbol{W_2}$	$\boldsymbol{W_3}$	$\boldsymbol{W_4}$	$\Delta \boldsymbol{E}^{\ddagger}_{for}$	$\Delta \boldsymbol{E}^{\ddagger}_{rev}$	$\Delta \boldsymbol{E}_{rxn}$	$\Delta \boldsymbol{E}$
14.0	5.2	-33.0	-31.7	19.2	64.7	-45.6	-45.4

All values are reported in kcal mol^{-1}. $\boldsymbol{W_n}$ is the amount of work associated with each of the *n* zones along with the IRC. $\Delta \boldsymbol{E}^{\ddagger}_{for}$ and $\Delta \boldsymbol{E}^{\ddagger}_{rev}$ are the activation energies. $\Delta \boldsymbol{E}_{rxn}$ is the reaction energy calculated by the integration of the Reaction Force (Eq. 1.17), and $\Delta \boldsymbol{E}$ is the total energy calculated as the difference of the energies of the frequencies calculations from stationary states.

First, it is apparent from Figure 3.3.4. that before ξ=-8.0 a.u. the change in energy is negligible. In means that the fragments do not have any structural or electronic rearrangements, they are just approaching each other. This is also evident in the evolution of the selected descriptors (C-C bond distances, bond orders, and atomic charges), which do not change in this region, except for the C1-C3 and C2-C6 distances.

Note that the energy slightly increases until ξ=-1.46 a.u. (coordinate where the transition state region begins) or, in other words, when the C1-C3 and C2-C6 distances are 1.85 Å. At this moment, everything takes place. Concomitantly, while C1-C3 and C2-C6 bonds are formed (moving away from 1.85 to 1.50 Å), the C1-C2, C3-C4, and C5-C6 bond distances increase roughly from 1.30 to 1.50 Å and the C4-C5 bond distances decrease from 1.50 to 1.30 Å. The evolution of bond distances goes hand in hand with the changes in the bond orders. Clearly, the WBIs reinforce the formation of single bonds between C1-C3 and C2-C6, the change of double to single bonds for C1-C2, C3-C4, and C5-C6, and the creation of a double bond between C4 and C5.

Changes in electronic distribution also follow the previous geometrical changes. The most noticeable difference occurs in C3 and C6, which accept 0.12 |e|. The pair C1 and C2 also accept a charge but in a smaller amount (just 0.02 | e |). That is, the carbon atoms involved in the formation of the new bonds accept a charge, while the C4 and C5 carbons only lose 0.03 | e |. The hydrogen atoms donate the rest of the charge to the carbon skeleton.

3.3.2. Electrocyclization of 1,3,5-hexatriene to 1,3-cyclohexadiene

As shown in Figure 3.3.6, the 1,3,5-hexatriene structure has a typical single (1.478 Å) bond length between C4 and C5, and double (1.332 Å and 1.343 Å) bond lengths in C5-C6 and C3-C4, respectively. The distance between C1 and C6 reduces from 3.397 Å to 2.271 Å in TS structure, close to the value reported in the literature at BLYP/6-31G (2.299 Å).[74]

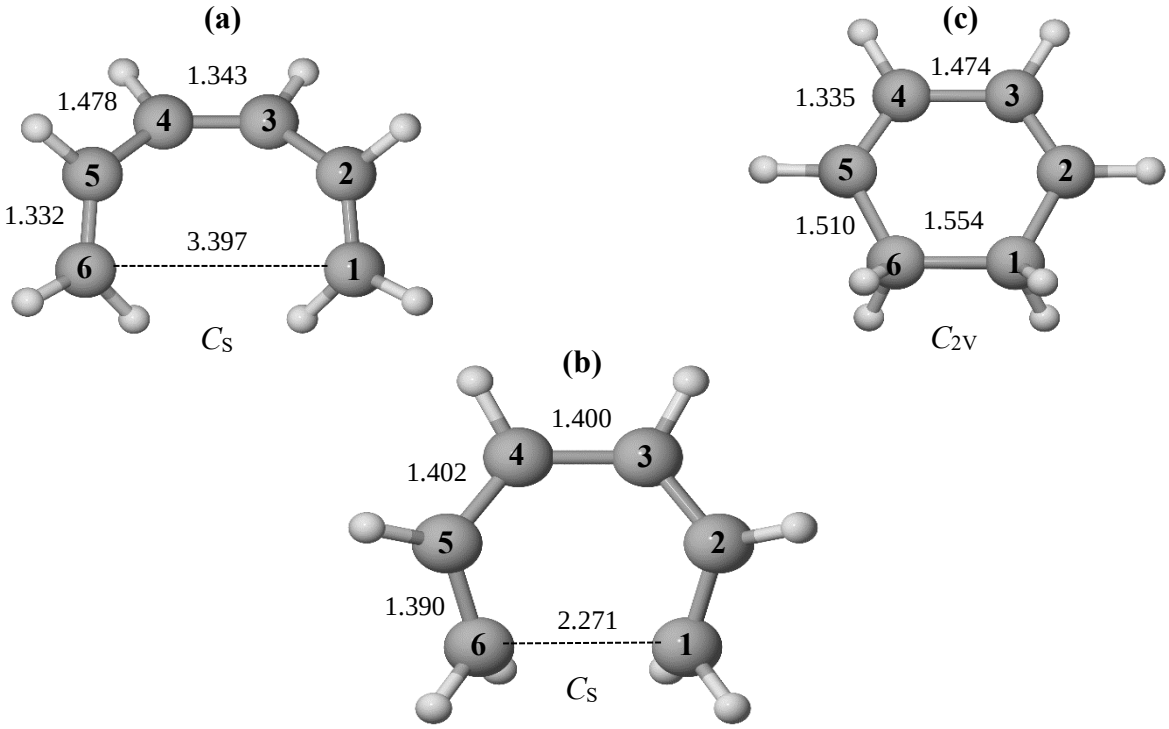

Figure 3.3.6. The M11/6-31+G(d,p) geometries of **(a)** 1,3,5-hexatriene, **(b)** transition state, and **(c)** 1,3-cyclohexadiene of electrocyclization. Bond lengths are shown in Angstroms.

To verify that the captured TS connects with the two minima, the IRC calculations were performed. It was expected that on the side of the reactant the IRC leads us directly to C_2 1,3,5-hexatriene, and on the side of the product leads us to C_2 1,3-cyclohexadiene. Nevertheless, the IRC on the reactant's side stops in the C_S 1,3,5-hexatriene, and on the product's side stops in C_{2v} 1,3-cyclohexadiene (Figure 3.3.7). It means that, at least at the M11 level, the electrocyclization of 1,3,5-hexatriene to 1,3-cyclohexadiene involves at least three steps, first the hexatriene isomerization, second the hexatriene electrocyclization, and third the cyclohexadiene isomerization.

The typical experimental energy barrier reported for the electrocyclization of 1,3,5-hexatriene to 1,3-cyclohexadiene is 29.0 kcal mol^{-1} in the gas phase.[71-72] In our case, $\Delta G^{\ddagger}$ is 21.6 kcal mol^{-1} computed at the M11 level. Theoretical value of $\Delta E^{\ddagger}$ is reported to be 20.7 kcal mol^{-1} at B3LYP/6-311++G(d,p) level, which is comparable with the value reported in this work (21.0 kcal mol^{-1}).

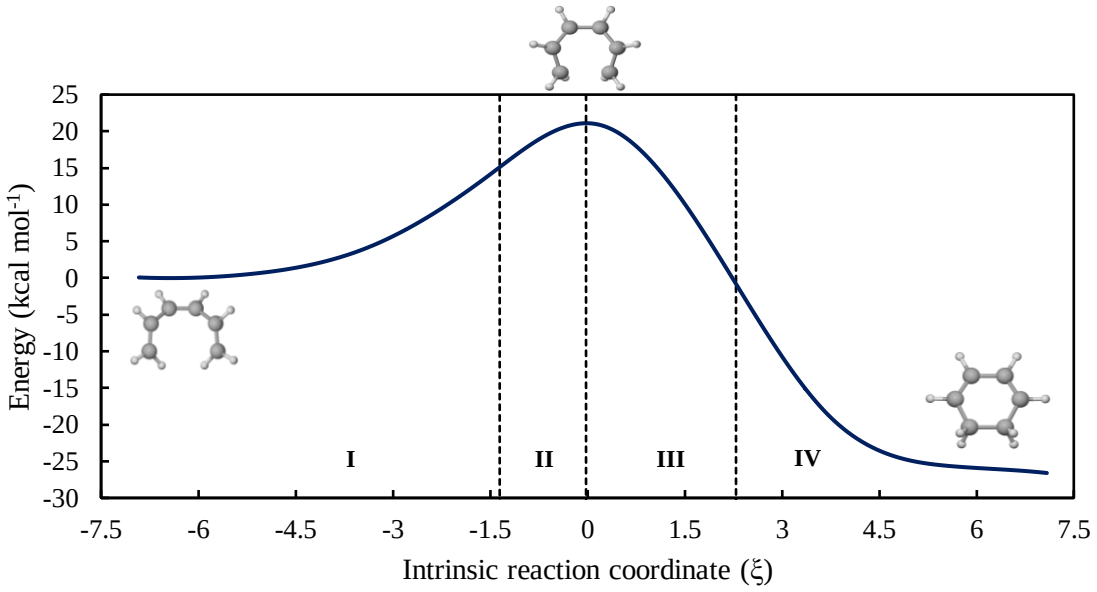

Figure 3.3.7. V(ξ) profile in kcal mol^{-1} of the electrocyclization of 1,3,5-hexatriene to 1,3-cyclohexadiene. Reactants, TS, and product structures of the reaction at M11/6-31+G(d,p) level are shown. The dashed vertical lines delimit the reactant region (I), transition state region (II and III), and product region (IV).

The F(ξ) profile provides a division along with the IRC. Herein, ξ = -1.35 and ξ = 2.29 delimit the TS region. The energetics recovered by the integration of the reaction force profile is reported in Table 3.3.3. Note that the reaction energy (ΔE_{rxn}) computed by the integration of the reaction force (-26.7 kcal mol^{-1}) is 0.3 kcal mol^{-1} lower than ΔE calculated as the difference of the energies between reactants and products, validating the module.

Table 3.3.3. Energy quantities associated with the electrocyclization of 1,3,5-hexatriene to 1,3-cyclohexadiene computed at the M11/6-31+G(d,p) level.

W_1	W_2	W_3	W_4	$\Delta E^{\ddagger}_{for}$	$\Delta E^{\ddagger}_{rev}$	ΔE_{rxn}	ΔE
15.0	6.0	-21.9	-25.8	21.0	47.7	-26.7	-26.4

All values are reported in kcal mol^{-1}. W_n is the amount of work associated with each of the *n* zones along with the IRC. $\Delta E^{\ddagger}_{for}$ and $\Delta E^{\ddagger}_{rev}$ are the activation energies. ΔE_{rxn} is the reaction energy calculated by the integration of the Reaction Force (Eq. 1.17), and ΔE is the total energy calculated as the difference of the energies of the frequencies calculations from stationary states.

It is apparent from Figure 3.3.8 b that before ξ=-1.35 there is a close-up between atoms C1 and C6, a recognition is happening between these two atoms. The energy slightly increases until ξ=-1.35, where the TS region begins, when C1-C6 distance is 2.50 Å. At this moment, and through the TS region, every big structural rearrangement and electronic change take place. While C1-C6 bond is formed (moving away from 3.40 Å to 1.55 Å) and gaining the simple-bond character at ξ=-2.29, the C1-C2, C3-C4, and C5-C6 double bonds distances increase from 1.33 Å to 1.50 Å, and the C2-C3 and C4-C5 distances decrease from 1.57 Å to 1.33 Å. WBI profile (Figure 3.3.8 c) reinforce the formation of new simple bond between C1-C6 (changing from 0.0 to 1.0) , and the formation of double bonds C2-C3 and C4-C5 (changing their WBI from 1.06 to 1.88).

Change in electronic distribution is like the previous geometrical changes (Figure 3.3.8 d). The biggest change in electronic distribution is in atoms C1 and C6, which accept 0.1 |e|. while C2 and C5 accept a smaller amount, 0.06 |e|. C3 and C4 only lose 0.03 |e|. Carbons involve in the formation of the new bond accept charge from the other carbon atoms and from the hydrogen atoms.

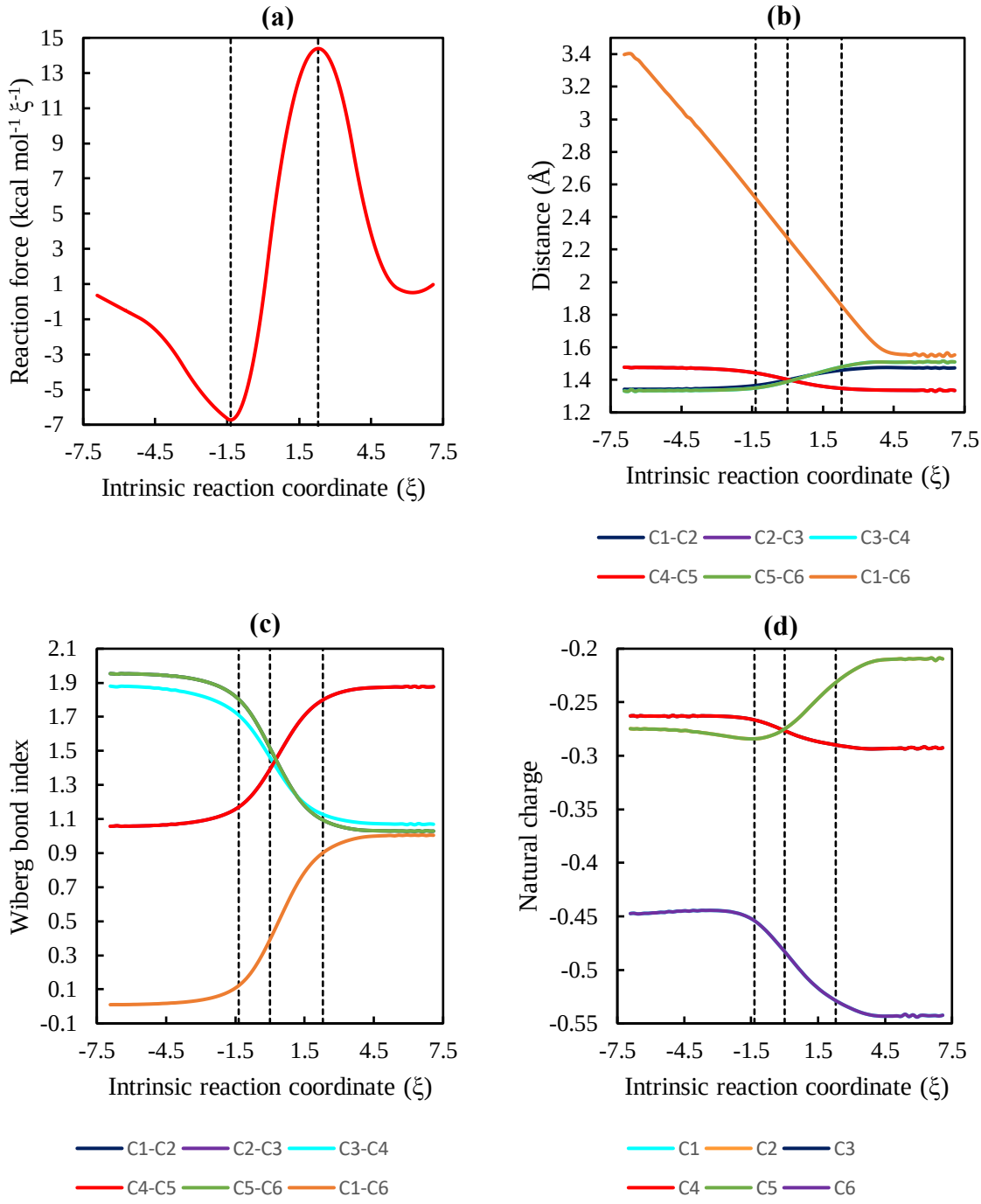

Figure 3.3.8. (a) F(ξ) in kcal mol^{-1} ξ^{-1}, **(b)**, evolution of all relevant bonds, **(c)** Wiberg bond indices, and **(d)** natural charges profiles of the carbon atoms of the electrocyclization of 1,3,5-hexatriene to 1,3-cyclohexadiene. The dashed vertical lines delimit the different regions. From left to right, the delimited zones are reactant region (I), transition state region (II and III), and product region (IV).

3.3.3. Degenerate [3,3] Cope rearrangement of 1,5-hexadiene

The degenerate [3,3] Cope rearrangement of 1,5-hexadiene proceeds via an aromatic chair-like transition structure (Figure 3.3.9). The C_{2h} (chair) transition structure for the Cope rearrangement at M11/6-31+G(d,p) level is shown in Figure 3.3.10, where C1-C2 and C4-C5 atoms have a distance between them of 1.952 Å between. This similitude in the C1-C2 and C4-C5 distance indicates a synchronous pathway.

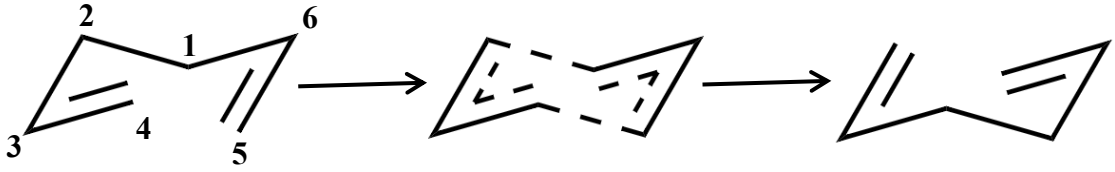

Figure 3.3.9. Degenerate [3,3] Cope rearrangement of 1,5-hexadiene via an aromatic TS.

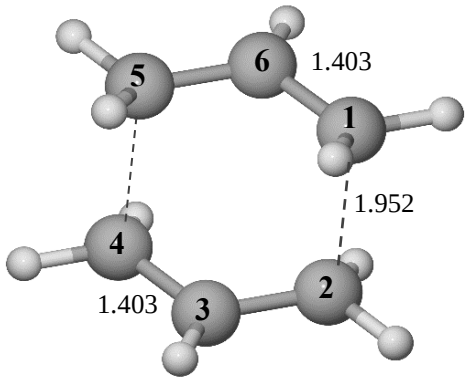

Figure 3.3.10. Transition state corresponding to the degenerate [3,3] Cope rearrangement of 1,5-hexadiene. Bond lengths are shown in Angstroms.

The experimental energy barrier reported for the degenerate [3,3] Cope rearrangement of 1,5-hexadiene is 33.5 kcal mol^{-1}.[75] In our case, the relative enthalpy energy between the TS and 1,5-hexadiene ($\Delta H^{\ddagger}$) is 33.0 kcal mol^{-1} computed at the M11 level, very similar to the experimental reported value.

To verify the TS, IRC calculations were performed, connecting with 1,5-hexadiene on the product and reactant sides (see Figure 3.3.11). Having the same structures on both sides of the IRC is reflected in the V(ξ) profile, which has a symmetrical behavior.

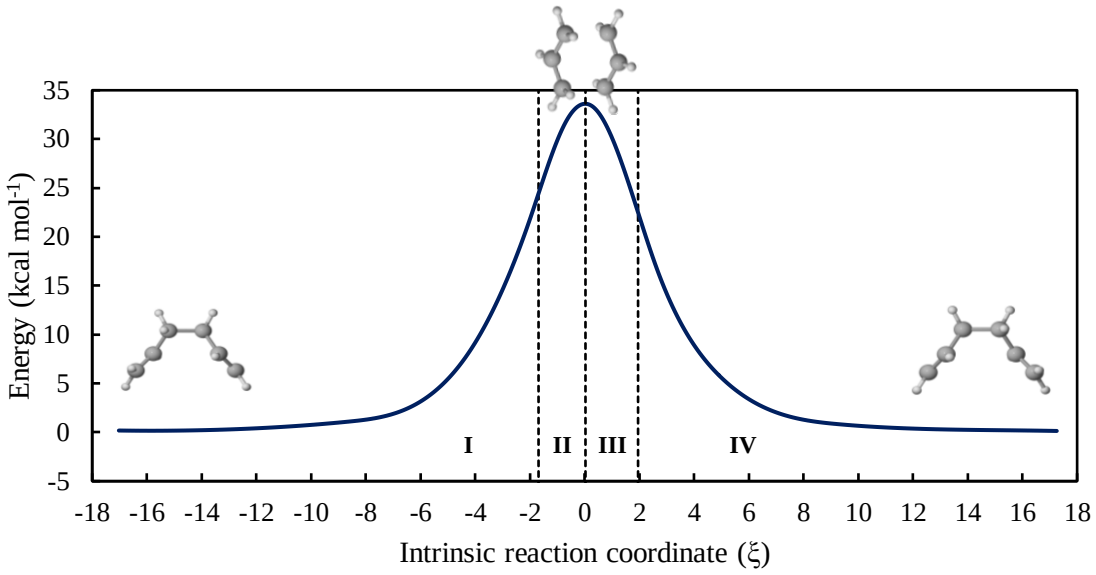

Figure 3.3.11. V(ξ) profile in kcal mol^{-1} of the degenerate [3,3] Cope rearrangement of 1,5-hexadiene. Reactants, TS, and product structures of the reaction at M11/6-31+G(d,p) level are shown. The dashed vertical lines delimit the reactant region (I), transition state region (II and III), and product region (IV).

The reaction force provides a natural division along with the IRC (see Chapter 1), the amount of work necessary in each of these zones (recovered by the integration of the reaction force profile) are presented in Table 3.3.4. The reaction energy ($\Delta \boldsymbol{E}_{\boldsymbol{rxn}}$) computed by the integration of the reaction force is equal to the difference of the energies between reactants and products (0.0 kcal mol^{-1}).

Table 3.3.4. Energy quantities associated with the degenerate [3,3] Cope rearrangement of 1,5-hexadiene computed at the M11/6-31+G(d,p) level.

$\boldsymbol{W_1}$	$\boldsymbol{W_2}$	$\boldsymbol{W_3}$	$\boldsymbol{W_4}$	$\Delta \boldsymbol{E}^{\ddagger}_{\boldsymbol{for}}$	$\Delta \boldsymbol{E}^{\ddagger}_{\boldsymbol{rev}}$	$\Delta \boldsymbol{E}_{\boldsymbol{rxn}}$	$\Delta \boldsymbol{E}$
24.3	9.2	-11.1	-22.4	33.5	33.5	0.0	0.0

All values are reported in kcal mol^{-1}. $\boldsymbol{W_n}$ is the amount of work associated with each of the *n* zones along with the IRC. $\Delta \boldsymbol{E}^{\ddagger}_{\boldsymbol{for}}$ and $\Delta \boldsymbol{E}^{\ddagger}_{\boldsymbol{rev}}$ are the activation energies. $\Delta \boldsymbol{E}_{\boldsymbol{rxn}}$ is the reaction energy calculated by the integration of the Reaction Force (Eq. 1.17), and $\Delta \boldsymbol{E}$ is the total energy calculated as the difference of the energies of the frequencies calculations from stationary states.

The F(ξ) and κ(ξ) profile are shown in Figure 3.3.12. The κ(ξ) profile provides a better idea about the synchronicity/nonsynchronicity of the reactions.[56-57, 76] It has been shown that κ(ξ) in the TS region is a sensitive indicator of the degree of synchronicity of a concerted reaction: a single minimum in κ(ξ) indicates a fully synchronous or nearly full synchronous, three critical points in the TS region means that the reaction proceeds in a significantly asynchronous, while a positive maximum between two minima represents extremely asynchronous reactions.[69] So, the κ(ξ) profile of the degenerate [3,3] Cope rearrangement of 1,5-hexadiene with just one minimum at the TS region means that this reaction happens in synchronous mode.

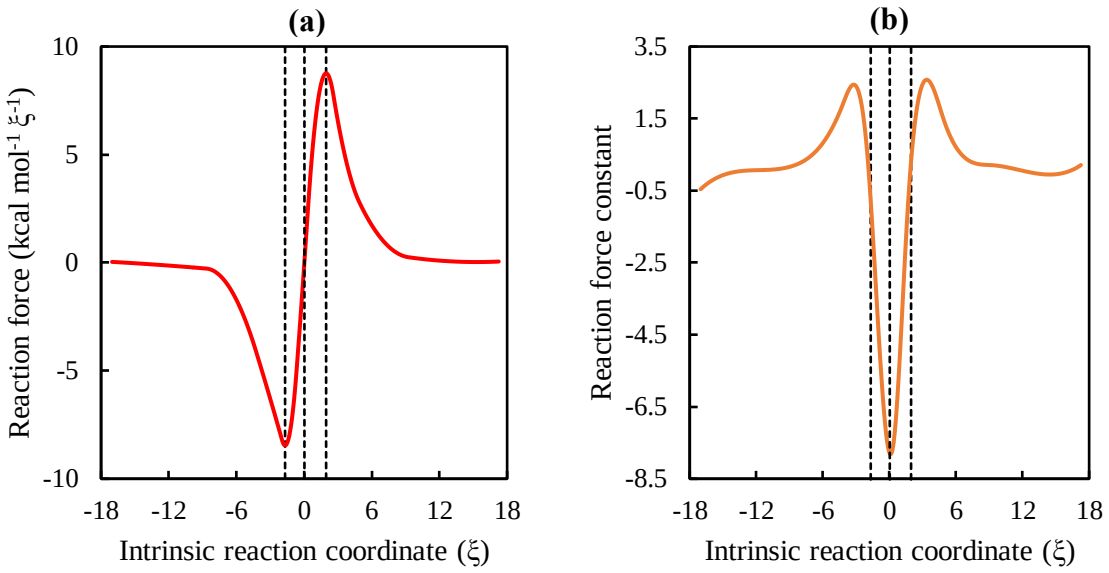

Figure 3.3.12. (a) F(ξ) in kcal mol^{-1}, and **(b)** κ(ξ) profiles of the degenerate [3,3] Cope rearrangement of 1,5-hexadiene. The dashed vertical lines indicate the limits of the different zones along the IRC. From left to right, the delimited zones are reactant region (I), transition state region (II and III), and product region (IV).

For a better understanding of the reaction mechanism, the evolution of the C-C distances, the corresponding WBI, and the atomic changes for the degenerate [3,3] Cope rearrangement of 1,5-hexadiene are shown in Figure 3.3.13.

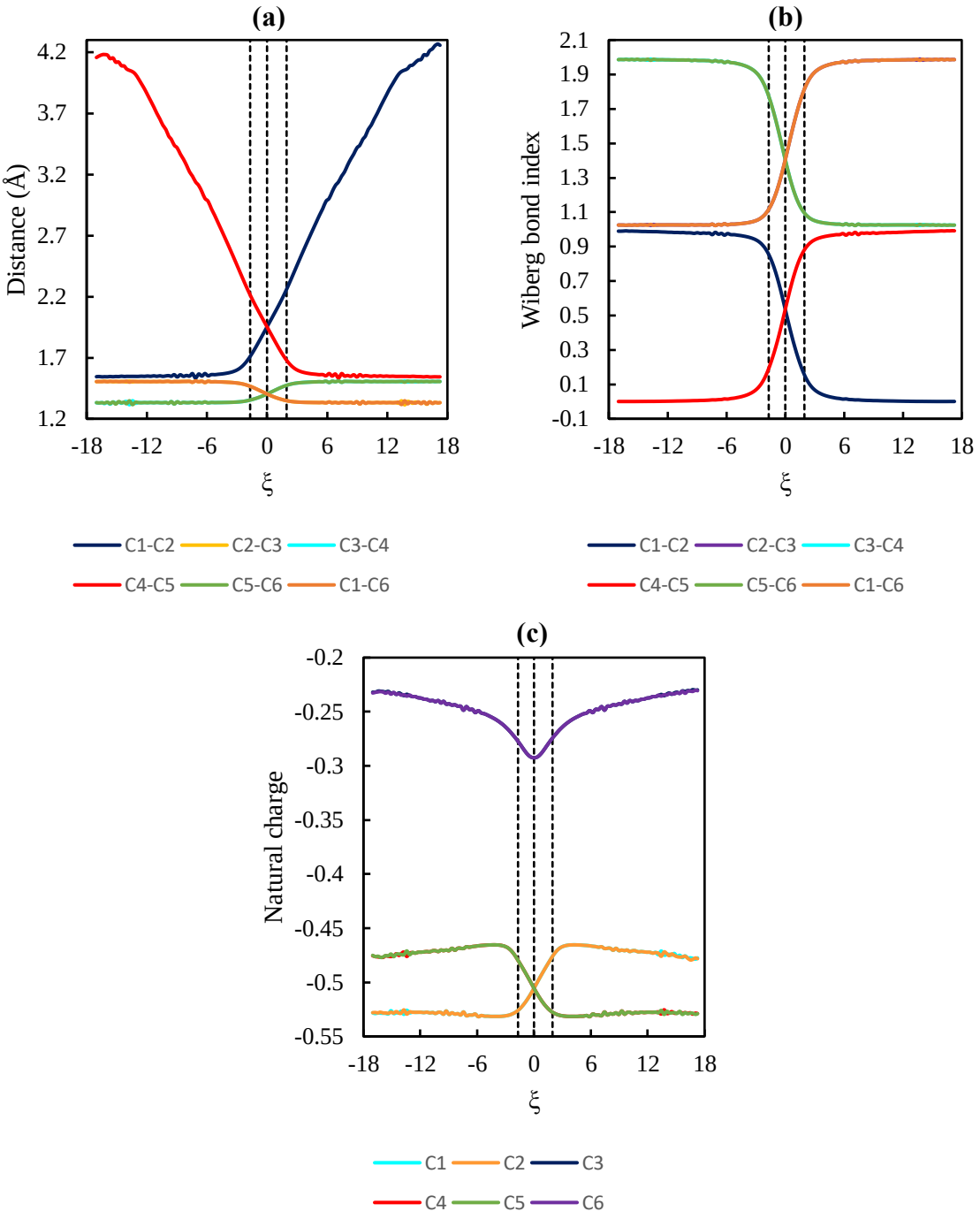

Figure 3.3.13. (a) Evolution of all relevant bonds, and **(b)** Wiberg bond indices, and **(c)** natural charges profiles of the carbon atoms of the degenerate [3,3] Cope rearrangement of 1,5-hexadiene. The dashed vertical lines delimit the different regions. From left to right, the delimited zones are reactant region (I), transition state region (II and III), and product region (IV).

The major approach between C4 and C5 atoms occurs in the first region. At ξ=-1.68, when the TS region begins, the structural rearrangements in C-C bonds start to take place: the distance between carbon atoms in single bonds (C2-C3 and C1-C6) decrease from 1.50 Å to 1.33 Å, while atoms C1 and C2 separate to break the single bond (changing their distance from 1.54 Å to 4.25 Å), opposite to change between C4-C5 atoms. Distances between C3-C4 and C5-C6 increase from 1.33 Å to 1.50 Å. The distances and the WBI profiles go hand by hand to explain the formation and breaking of single and double bonds along with the reaction. The new formed single bond (C4-C5) change their bond order from 0.0 to 1.0, single bonds C2-C3 and C1-C6 change their bond order from 1.02 to 1.98, C3-C4 and C5-C6 lose their double-bond character changing from 1.98 to 1.02, while C1 and C2 change bond order from 1.0 to 0.0, meaning that the bond is breaking.

Charges distributions have a similar trend that WBI profile. C4 and C5 gain 0.05 |e|, while C1 and C2 lose the same amount. C3 and C6 change their natural charge but in the end, it recovers the same value of -0.23 |e|. The TS is characterized by the biggest electronic delocalization. From these, we can note that the electron changes in the carbon skeleton are composed by themselves. The biggest electronic reorganization between carbon atoms begins to take place near to the reaction force minima, ξ=-1.68, and through the TS region, when structural rearrangements are happening.

3.3.4. Double group transfer from ethane to ethylene

The archetypal DGT reaction between ethane and ethylene is the synchronous transfer of two hydrogen atoms, from ethane to ethylene, which occurs through the highly symmetric planar six-membered ring transition structure. The transition structure for the Cope rearrangement at M11/6-31+G(d,p) level is shown in Figure 3.3.14. Significantly, the equalized CC bond distances have partial double-bond character thereby satisfying the geometric criterion for aromaticity. The distance between donor/receptor atoms and hydrogens is 1.369 Å, and the distance between carbon atoms in partial double bonds is 1.416 Å, these values are comparable with those reported in the literature at B3LYP/def2-TZVPP level (1.372 Å and 1.416 Å, respectively).

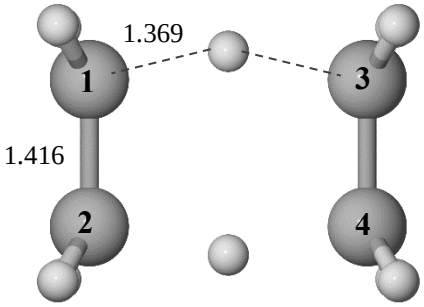

Figure 3.3.14. Transition state corresponding to the archetypical DGT reaction between ethane and ethylene. Bond lengths are shown in Angstroms.

To verify that the captured TS connects with the two minima, the IRC calculations were performed. These lead us directly to ethane + ethylene on both sides of the reaction. The reactant and product structures at M11 level are shown in Figure 3.3.15. The relative free energy ($\Delta H^{\ddagger}$) between TS and 1,3,5-hexatriene, computed in this work at the M11 level, is 57.6 kcal mol^{-1}, which is comparable with the theoretical value reported at B3LYP/def2-TZVPP level (58.2 kcal mol^{-1}).[77]

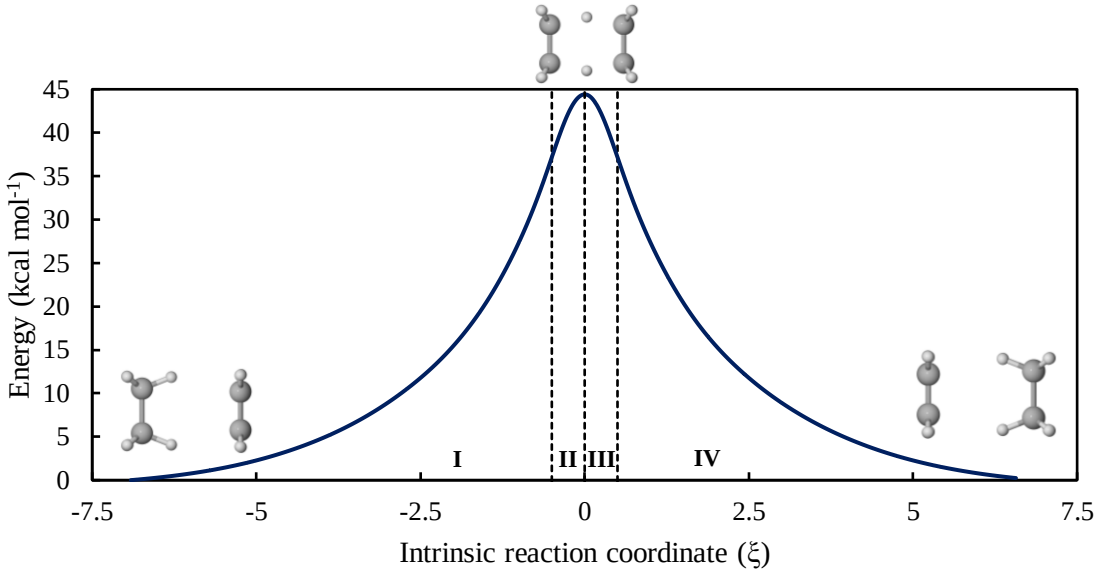

Figure 3.3.15. V(ξ) profile in kcal mol^{-1} of the DGT reaction between ethane and ethylene. Reactants, TS, and product structures of the reaction at M11/6-31+G(d,p) level are shown.. The dashed vertical lines delimit the reactant region (I), transition state region (II and III), and product region (IV).

Now, let us analyze the variation of some descriptors (as bond distances, WBIs, and atomic charges) along the IRC to try to understand the DGT reaction in detail and to validate the *Reaction Force module*. The F(ξ) and κ(ξ) are shown in Figure 3.3.16. The evolution of some atom distances, the corresponding WBI, and the atomic changes for the DGT reaction between ethane and ethylene are depicted in Figure 3.3.17.

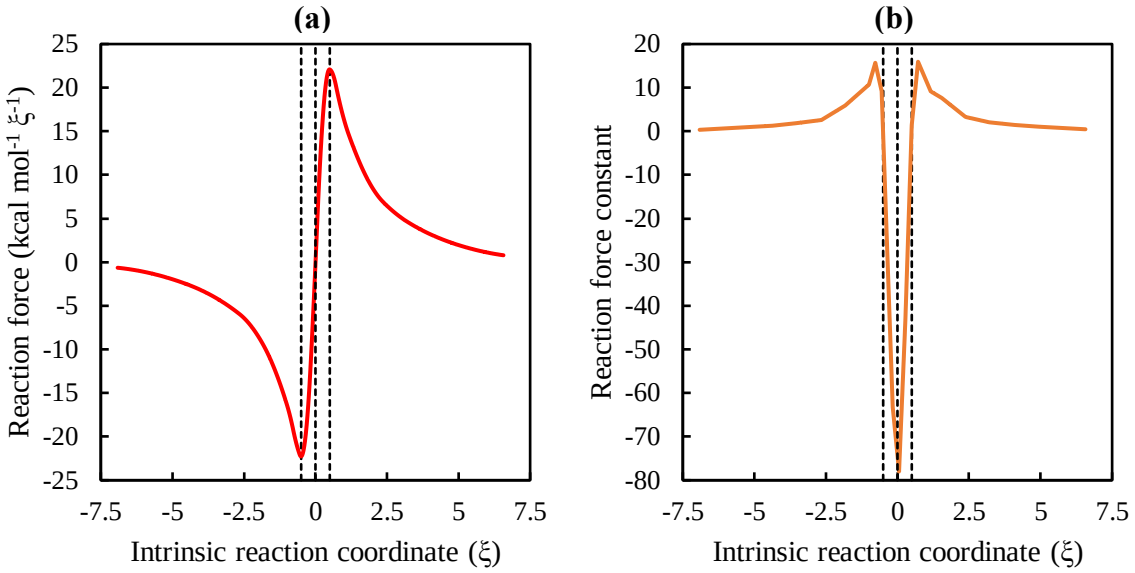

Figure 3.3.16. (a) F(ξ) in kcal mol^{-1}, and **(b)** κ(ξ) profiles of the DGT reaction between ethane and ethylene. The dashed vertical lines delimit the different regions. From left to right the delimited zones are reactant region (zone 1), transition state region (zones 2 and 3), and product region (zone 4).

Table 3.3.5. Energy quantities associated with the archetypical DGT reaction between ethane and ethylene computed at the M11/6-31+G(d,p) level.

$\boldsymbol{W_1}$	$\boldsymbol{W_2}$	$\boldsymbol{W_3}$	$\boldsymbol{W_4}$	$\Delta\boldsymbol{E}^{\ddagger}_{for}$	$\Delta\boldsymbol{E}^{\ddagger}_{rev}$	$\Delta\boldsymbol{E}_{rxn}$	$\Delta\boldsymbol{E}$
37.2	7.0	-7.0	-37.2	44.2	44.2	0.0	0.0

All values are reported in kcal mol^{-1}. $\boldsymbol{W_n}$ is the amount of work associated with each of the *n* zones along with the IRC. $\Delta\boldsymbol{E}^{\ddagger}_{for}$ and $\Delta\boldsymbol{E}^{\ddagger}_{rev}$ are the activation energies. $\Delta\boldsymbol{E}_{rxn}$ is the reaction energy calculated by the integration of the Reaction Force (Eq. 1.17), and $\Delta\boldsymbol{E}$ is the total energy calculated as the difference of the energies of the frequencies calculations from stationary states.

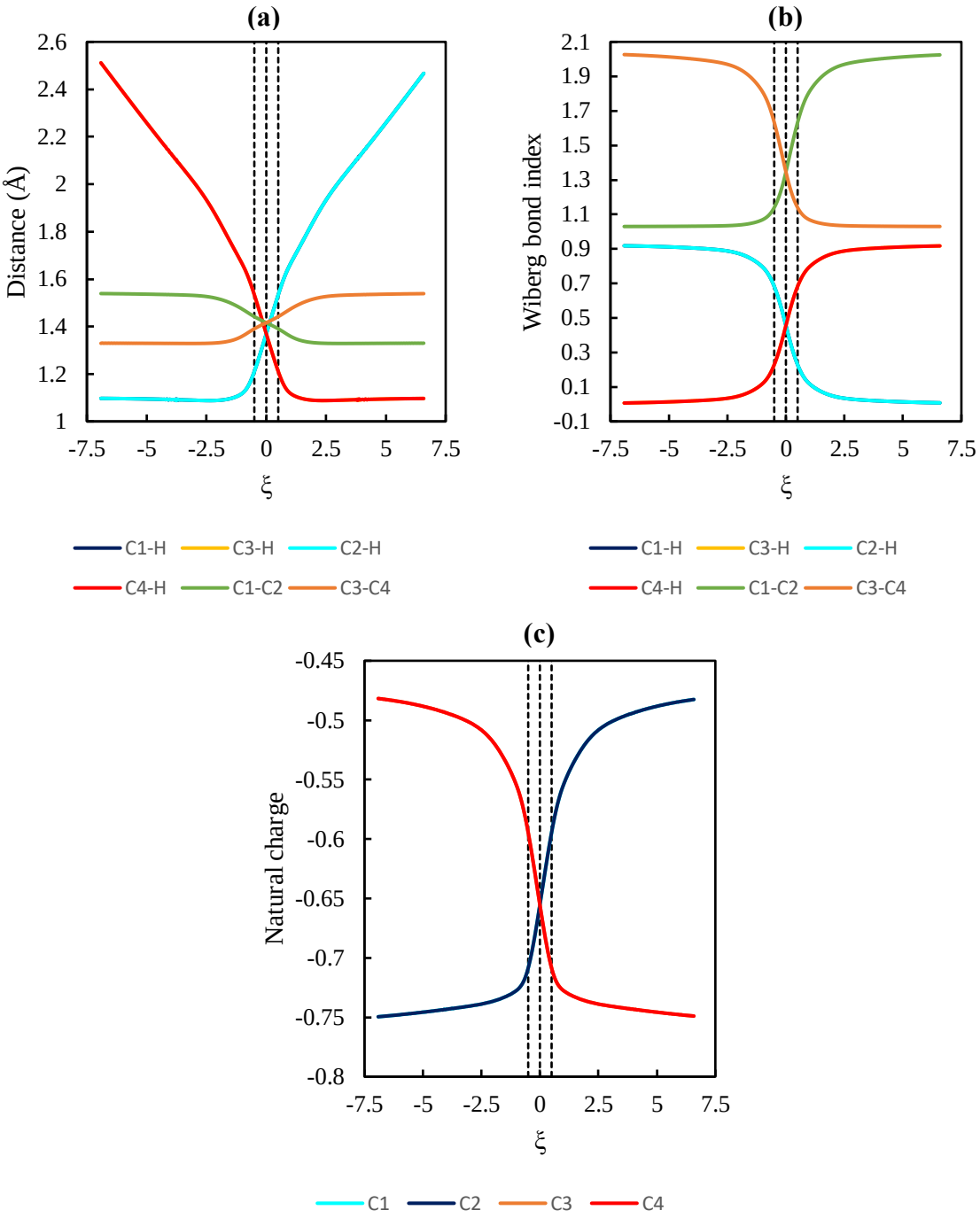

Figure 3.3.17. (a) Evolution of all relevant bonds, **(b)** Wiberg bond indices, and **(c)** natural charges profiles of the relevant atoms of the DGT reaction between ethane and ethylene. The dashed vertical lines delimit the different regions. From left to right, the delimited zones are reactant region (I), transition state region (II and III), and product region (IV).

The F(ξ) profile for the DGT reaction between ethane and ethylene is shown in Figure 3.3.16 a. The reaction force provides a natural division along with the IRC (see Chapter 1). This division let us perform an energy decomposition into each of the reaction force zones. The recovered amounts of energy by the integration of the reaction force profile are presented in Table 3.3.5. The reaction energy ($\Delta \boldsymbol{E}_{\boldsymbol{rxn}}$) computed by the integration of the reaction force is equal to the difference of the energies between reactants and products (0.0 kcal mol^{-1}), which validate the *Reaction Force module*.

On the other hand, κ(ξ) profile is an indicator of the level of synchronicity in a reaction. As we can see in Figure 3.3.16 b, the κ(ξ) profile of the DGT reaction between ethane and ethylene presents only a minimum in the transition regions, which means that this reaction proceeds in a synchronous pathway.

Unlike the previous reaction, the energy V(ξ) kept constantly increasing in the first region, while the hydrogen atoms get close to the receptor carbons (C3 and C4). The bonds distance C3-C4 increase from 1.33 to 1.54 Å, whereas the bond distance C1-C2 decrease from 1.54 to 1.33 Å, when going from reactants to products. This is due in the first case (C3-C4) to the loss of the double-bond character (changing from 2.02 to 1.03 their Wiberg bond index) and in the second case (C1-C2) to the gain of the double-bond character (changing from 1.03 to 2.02 their WBI)

Figure 3.3.17 a. displays the variation of the distance between the donor (C1 and C2) and acceptor (C3 and C4) atoms with the hydrogens being transferred along with the IRC. It is noted that the C3-H and C4-H distances decrease from reactants (2.51 Å) to products region's limit at ξ=0.50, thereafter they remain practically constant until the distance between these atoms is 1.10 Å. Interestingly, in the reactant region, the C1-H and C2-H remain constant. The C3-H and C4-H gain the single-bond character, changing their WBI from 0.0 to 0.92, and the C1-H and C2-H lose it, changing their WBI from 0.0 to 0.92, along with the IRC from reactants to products (Figure 3.3.17 b).

Natural charge profiles of the carbon atoms in the DGT reaction between ethane and ethylene are shown in Figure 3.3.17 c, which have a similar trend to the WBI profile. C3 and C4 atoms gain 0.27 |e|, while C1 and C2 lose the same amount. This means that the losing and gaining of electrons in the carbon skeleton is compensated by themselves.

From all these analyses of the four pericyclic reactions, we can assume, that the first region of the reaction force is characterized by recognition between the fragments (or molecules) involved in the reaction. When the reaction force minimum is reached, the charge transfer between atoms, and structural arrangements take place. The transition region is characterized by the breaking and formation of bonds. All electronic and structural changes end at the maximum of the reaction force. The product region is characterized by a relaxing in the molecules to form the product structures.

CONCLUSIONS AND PERSPECTIVES

In this work, a new module in *Eyringpy*, called *Reaction Force*, has been introduced. The main idea of this new implementation is to perform energy and properties analysis decomposition in elementary reactions using the Reaction Force theory. In this version, a spline interpolator has been programmed and implemented to smooth energy, reaction force, and reaction force constant profiles. The properties available to be analyzed in this version are bond distances, Wiberg bond indices, natural charges, dipole moments, and HOMO-LUMO bandgap. The internal structure in subroutines of the *Reaction Force module* lets easily to do new implementations in it.

Reaction Force module is an easy tool to perform reaction mechanism analysis, thanks to its user-friendly interface. The short compute time helps the user to perform a complete analysis in seconds, which is helpful when a comparison between different reaction mechanism carry out. A plotter has been programmed and implemented to easily visualize the behavior of the analyzed data. Another advantage of this module is that the data is processed automatically, eliminating the human errors. No more spreadsheets!

The analysis of structural and electronic properties along with the IRC helps to understand the changes in the molecules involved in a reaction mechanism. This has been proved by the analysis of four pericyclic reactions, the Diels-Alder reaction between *s-cis*-butadiene and ethylene, the electrocyclization of 1,3,5-hexatriene to 1,3-cyclohexadiene, the degenerate [3,3] Cope rearrangement of 1,5-hexadiene, and the double group transfer between ethane and ethylene. The results obtained by the *Reaction Force module* helped to have a better understanding of these reaction mechanisms. It was found that these four reactions are characterized by having a closeness between the molecules (or fragments) throughout the region of the reactants, in the transition region, the most important structural and electronic rearrangements are carried out, while the region of the products is characterized by a structural relaxation.

Future versions will include new interpolator options, such as Lagrange and Taylor polynomial interpolations. The main idea of including more than one interpolator option is to allow the user to choose the one that best suits the behavior of the reaction's energy profile.

New properties available to be analyzed throughout IRC will be implemented in future versions, such as angles, dihedral angles, multipole moments, molecular orbital occupations, orbital energies, etc. These new implementations will help the user to have more detailed analysis of the reaction mechanisms.

Energy Decomposition Analysis (EDA) and Activation Strain Model (ASM) will be implemented. These implementations allow the user to compare between different reactivity models and choose the one that best suits the reaction of interest.

Appendix A. Code

Reaction Force module is available in *Eyringpy* 1.1 and higher versions.

Eyringpy 1.1 is available for downloading through the Merino Research Group. To obtain a copy of *Eyringpy*, go to TheoChem's web page: **www.theochemmerida.org** and follow the steps to receive an executable compatible with the operating system that you required.

Appendix B. Constant values and unit conversion

Table B1. Fundamental Physical Constants employed in *Eyringpy*.

Constant name	Symbol	Value	Units
Atomic mass constant	m_u	1.66053906660 x 10^{-27}	kg
Avogadro constant	N_A	6.02214076 x 10^{23}	mol^{-1}
Bohr radius	a_o	5.29177210903 x 10^{-11}	M
Boltzmann constant	k	1.380649 x 10^{-23}	J K^{-1}
Molar constant gas	R	8.314462618	J mol^{-1} K^{-1}
Planck constant	h	6.62607015 x 10 -34	J Hz^{-1}
Reduced Planck constant	$\hbar$	1.054571817 x 10^{-34}	J s
Standard-State Pressure	*ssp*	100 000	Pa
Speed of light	c	299 792 458	m s^{-1}

Table B2. Unit conversion employed in *Eyringpy*.

Value	Equivalence
1 Å	1 x 10^{-10} m
1 cal	4.184 J
1 m^3	1000 L
1 Ha	4.359744650 x 10^{-18} J

Appendix C. User Manual

Content

C1. System requirements and installation

C2. Input file

C3. Run an example

C1. System requirements and installation

Eyringpy is compatible with Linux, Mac Os and Windows. It is necessary to create a folder and place the executable program, eyringpy.exe, in it. An input file with the name of the folder and eif termination (foldername.eif) must be created and placed it in the same folder as the executable program.

C2. Inputfile

The *Eyringpy* input file, foldername.eif, requires three types of input data, related to specific keywords, which are described in Chapter 2. They can appear in any order and are not case-sensitive. The first set is composed by frequency and IRC output files of the species involved in the reaction: transition state, reactant(s), product(s), and IRC calculations. The second set is composed by the interpolation specifications: type of interpolation, number of new points to generate, interpolation order, smooth factor and threshold to discriminate points from the potential energy curve. Third set is composed by properties analysis options: dipole moment, HOMO-LUMO gap, natural charges, bond lengths and Wiberg bond indices. A *Reaction Force* input file example is shown in Figure C2.1.

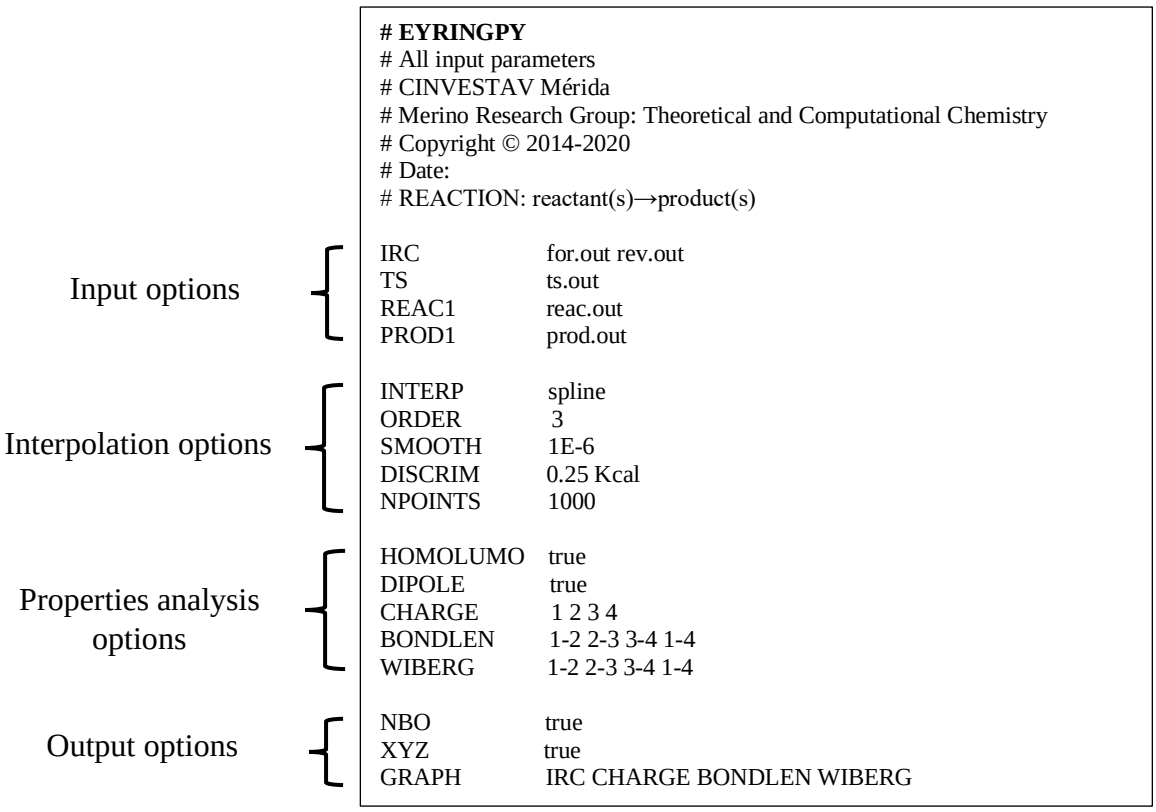

Figure C2.1. *Reaction Force* input file example.

C3. Run an example

To run a Reaction Force calculation in *Eyringpy* some steps must be follow, here they are listed below:

1. Create a folder and located the *Eyringpy* executable (Eyringpy.exe).
2. Locate *Gaussian* IRC and frequency calculations in the same folder.
3. *Reaction Force* input file must be named as the folder's name with eif termination (foldername.eif).

If an input file example must be created by the program, go to steps 7 and 8.

If property analysis is going to be required, follow steps 4 and 5. If not, go to step 6.

4. Create a folder named NBO in the same folder where the executable program is located.
5. NBO calculation file of each molecule geometry of the IRC must be in NBO folder. These files must be named as numbers (in order from left to right along the IRC) using at least three digits, e.g., 001.out, 002.out, 003.out, 004.out, etc. The number of NBO calculation files must be the same that the number of points along IRC.
6. Open the command prompt.
7. Go to the folder where the executable program is located by typing, for instance:

```
cd Documents\Programs\foldername\
```

8. Type eyringpy.exe

```
eyringpy.exe
```

   and a welcome-help message will be visualized.
9. If eyringpy.exe is run, and there is not an *Eyringpy* input file in the folder, the program will create an example. This input file example may be edited.
10. To run a Reaction Force calculation, type:

```
eyringpy.exe -rf
```

11. Open the *Reaction Force* output file(s).

If properties analysis were computed, an output file for each property was created, named as its keyword name and eof termination. Graphics are also named as the keyword property name and png termination.

Appendix D. Chapter 4 supporting information

D1. Cartesian coordinates of the transition states optimized at M11/6-31+G(d,p).

DA reaction between *s-cis*-1,3-butadiene and ethylene – TS:

6	-0.269585000	1.565938000	0.689069000
6	-0.269585000	1.565938000	-0.689069000
1	-1.199908000	1.421081000	1.236065000
1	0.524882000	2.076292000	1.235438000
1	-1.199908000	1.421081000	-1.236065000
1	0.524882000	2.076292000	-1.235438000
6	0.514162000	-0.442170000	1.421191000
6	-0.269585000	-1.316842000	0.706455000
1	0.416458000	-0.378029000	2.506434000
1	1.463192000	-0.089129000	1.019461000
1	-1.054573000	-1.871773000	1.225455000
6	-0.269585000	-1.316842000	-0.706455000
1	-1.054573000	-1.871773000	-1.225455000
6	0.514162000	-0.442170000	-1.421191000
1	1.463192000	-0.089129000	-1.019461000
1	0.416458000	-0.378029000	-2.506434000

Electrocyclization of 1,3,5-hexatriene to 1,3-cyclohexadiene – TS:

6	0.115899000	1.239671000	0.699973000
6	0.115899000	1.239671000	-0.699973000
1	0.032185000	2.220723000	1.174591000
1	0.032185000	2.220723000	-1.174591000
6	-0.207565000	0.112784000	1.469696000
1	-0.898445000	0.285580000	2.301703000
6	0.115899000	-1.196970000	1.135356000
1	1.150996000	-1.430846000	0.924786000
1	-0.430140000	-2.008364000	1.625249000
6	-0.207565000	0.112784000	-1.469696000
1	-0.898445000	0.285580000	-2.301703000
1	0.115899000	-1.196970000	-1.135356000
1	1.150996000	-1.430846000	-0.924786000
1	-0.430140000	-2.008364000	-1.625249000

Degenerate [3,3] Cope rearrangement of 1,5-hexadiene – TS:

6	0.263802000	-0.939866000	1.211439000
6	-0.263802000	0.939866000	1.211439000
6	0.263802000	1.412492000	0.000000000
6	-0.263802000	0.939866000	-1.211439000
6	0.263802000	-0.939866000	-1.211439000
6	-0.263802000	-1.412492000	0.000000000
1	0.174798000	1.297683000	2.146900000
1	-1.344776000	0.791412000	1.272660000
1	1.280669000	1.815751000	0.000000000
1	-1.344776000	0.791412000	-1.272660000
1	1.344776000	-0.791412000	-1.272660000
1	-1.280669000	-1.815751000	0.000000000
1	-0.174798000	-1.297683000	-2.146900000
1	0.174798000	1.297683000	-2.146900000
1	-0.174798000	-1.297683000	2.146900000
1	1.344776000	-0.791412000	1.272660000

DGT from ethane to ethylene – TS:

6	1.340077000	0.708043000	0.000000000
1	1.629703000	1.230990000	0.914458000
1	1.629703000	1.230990000	-0.914458000
1	0.000000000	0.989497000	0.000000000
6	1.340077000	-0.708043000	0.000000000
1	0.000000000	-0.989497000	0.000000000
1	1.629703000	-1.230990000	-0.914458000
1	1.629703000	-1.230990000	0.914458000
6	-1.340077000	0.708043000	0.000000000
6	-1.340077000	-0.708043000	0.000000000
1	-1.629703000	1.230990000	0.914458000
1	-1.629703000	1.230990000	-0.914458000
1	-1.629703000	-1.230990000	0.914458000
1	-1.629703000	-1.230990000	-0.914458000

REFERENCES

1. Shryock, R. H., A Guide to the History of Science: A First Guide for the Study of the History of Science with Introductory Essays on Science and Tradition. Oxford University Press: 1953.

2. Klippenstein, S. J.; Pande, V. S.; Truhlar, D. G., *J. Am. Chem. Soc.* **2014,** *136* (2), 528.

3. Fernández, I.; Bickelhaupt, F. M., *Chem. Soc. Rev.* **2014,** *43* (14), 4953.

4. Hopffgarten, M. v.; Frenking, G., *Wiley Interdiscip. Rev.: Comput. Mol. Sci.* **2012,** *2* (1), 43.

5. Toro-Labbé, A., *J. Phys. Chem. A* **1999,** *103* (22), 4398.

6. Vöhringer-Martinez, E.; Toro-Labbé, A., *J. Chem. Phys.* **2011,** *135* (6), 064505.

7. Toro-Labbé, A.; Gutiérrez-Oliva, S.; Murray, J.; Politzer, P., *Mol. Phys.* **2007,** *105* (19-22), 2619.

8. Politzer, P.; Toro-Labbé, A.; Gutiérrez-Oliva, S.; Murray, J. S., Perspectives on the reaction force. In *Adv. Quantum Chem.*, Elsevier: 2012; Vol. 64, pp 189.

9. Politzer, P.; Reimers, J. R.; Murray, J. S.; Toro-Labbé, A., *J. Phys. Chem. Lett.* **2010,** *1* (19), 2858.

10. Toro-Labbé, A.; Gutiérrez-Oliva, S.; Murray, J. S.; Politzer, P., *J. Mol. Model.* **2009,** *15* (6), 707.

11. Politzer, P.; Toro-Labbé, A.; Gutiérrez-Oliva, S.; Herrera, B.; Jaque, P.; Concha, M. C.; Murray, J. S., *J. Chem. Sci.* **2005,** *117* (5), 467.

12. Fukui, K., *Acc. Chem. Res.* **1981,** *14* (12), 363.

13. Fukui, K., *J. Phys. Chem.* **1970,** *74* (23), 4161.

14. Dzib, E.; Cabellos, J. L.; Ortíz-Chi, F.; Pan, S.; Galano, A.; Merino, G., *J. Quantum Chem.* **2019,** *119* (2), e25686.

15. Natta, G., *Elsevier, Amsterdam* **1972,** *27*, 3.

16. Chang, R.; Thoman, J. W., *Physical chemistry for the chemical sciences*. University Science Books: 2014.

17. Logan, S. R.; Pando García Pumarino, C., *Fundamentos de cinética química*. 2000.

18. Mortimer, M.; Taylor, P. G.; Taylor, P., *Chemical kinetics and mechanism*. Royal Society of Chemistry: 2002; Vol. 5.

19. Avery, H. E., *Basic reaction kinetics and mechanisms*. Macmillan International Higher Education: 1974.

20. McQuarrie, D. A.; Simon, J. D., *Physical chemistry: a molecular approach*. University science books Sausalito, CA: 1997; Vol. 1.

21. Elrod, M., An Introduction to Chemical Kinetics (Margaret Robson Wright). ACS Publications: 2005.

22. Arnaut, L.; Burrows, H., *Chemical kinetics: from molecular structure to chemical reactivity*. Elsevier: 2006.

23. Upadhyay, S. K., *Chemical kinetics and reaction dynamics*. Springer Science & Business Media: 2007.

24. Müller, K., *Angew. Chem., Int. Ed. Engl.* **1980,** *19* (1), 1.

25. Levine, I. N., *Physical Chemistry*. 6th ed ed.; McGraw-Hill: 2009; p 989.

26. Goldbook, I., *R05385. html (accessed May 8, 2014)*.

27. Cramer, C. J., *Essentials of computational chemistry: theories and models*. John Wiley & Sons: 2013.

28. Gonzalez, C.; Schlegel, H. B., *J. Phys. Chem.* **1990,** *94* (14), 5523.

29. Hratchian, H. P.; Schlegel, H. B., Finding minima, transition states, and following reaction pathways on ab initio potential energy surfaces. In *Theory Appl. Comput. Chem.: First Forty Years*, Elsevier: 2005; pp 195.

30. Dykstra, C.; Frenking, G.; Kim, K.; Scuseria, G., *Theory and applications of computational chemistry: the first forty years*. Elsevier: 2011.

31. Schlegel, H. B., *Trans. J* **1974,** *1339*, 1844.

32. Hratchian, H.; Schlegel, H., *J. Phys. Chem. A* **2002,** *106* (1), 165.

33. Hratchian, H.; Schlegel, H., *J. Chem. Theory Comput.* **2005,** *1* (1), 61.

34. Following the Intrinsic Reaction Coordinate. Ludwig Maximilians Universitat Munchen. http://www.cup.uni-muenchen.de.

35. Toro-Labbé, A.; Gutiérrez-Oliva, S.; Concha, M. C.; Murray, J. S.; Politzer, P., *J. Chem. Phys.* **2004,** *121* (10), 4570.

36. Martínez, J.; Toro-Labbé, A., *Chem. Phys. Lett.* **2004,** *392* (1-3), 132.

37. Yepes, D.; Murray, J. S.; Santos, J. C.; Toro-Labbé, A.; Politzer, P.; Jaque, P., *J. Mol. Model.* **2013,** *19* (7), 2689.

38. Duarte, F.; Vöhringer-Martinez, E.; Toro-Labbé, A., *Phys. Chem. Chem. Phys.* **2011,** *13* (17), 7773.

39. Lamsabhi, A. M.; Mó, O.; Gutiérrez-Oliva, S.; Pérez, P.; Toro-Labbé, A.; Yáñez, M., *J. Comput. Chem.* **2009,** *30* (3), 389.

40. Gutierrez-Oliva, S.; Herrera, B.; Toro-Labbe, A.; Chermette, H., *J. Phys. Chem. A* **2005,** *109* (8), 1748.

41. Rincon, E.; Jaque, P.; Toro-Labbe, A., *J. Phys. Chem. A* **2006,** *110* (30), 9478.

42. Herrera, B.; Toro-Labbe, A., *J. Phys. Chem. A* **2007,** *111* (26), 5921.

43. Herrera, B.; Toro-Labbe, A., *J. Chem. Phys.* **2004,** *121* (15), 7096.

44. Jaque, P.; Toro-Labbé, A., *J. Phys. Chem. A* **2000,** *104* (5), 995.

45. Herrera, B.; Toro-Labbé, A., *J. Phys. Chem. A* **2004,** *108* (10), 1830.

46. Vöhringer-Martinez, E.; Toro-Labbé, A., *J. Phys. Chem. A* **2012,** *116* (27), 7419.

47. Bulat, F.; Toro-Labbé, A., *Chem. Phys. Lett.* **2002,** *354* (5-6), 508.

48. Vogt-Geisse, S.; Toro-Labbé, A., *J. Chem. Phys.* **2009,** *130* (24), 244308.

49. Murray, J. S.; Toro-Labbé, A.; Clark, T.; Politzer, P., *J. Mol. Model.* **2009,** *15* (6), 701.

50. Politzer, P.; Murray, J. S.; Lane, P.; Toro-Labbé, A., *Int. J. Quantum Chem.* **2007,** *107* (11), 2153.

51. Politzer, P.; Burda, J. V.; Concha, M. C.; Lane, P.; Murray, J. S., *J. Phys. Chem. A* **2006,** *110* (2), 756.

52. Giri, S.; Echegaray, E.; Ayers, P. W.; Nuñez, A. S.; Lund, F.; Toro-Labbé, A., *J. Phys. Chem. A* **2012,** *116* (40), 10015.

53. Burda, J. V.; Murray, J. S.; Toro-Labbé, A.; Gutiérrez-Oliva, S.; Politzer, P., *J. Phys. Chem. A* **2009,** *113* (23), 6500.

54. Burda, J. V.; Toro-Labbe, A.; Gutierrez-Oliva, S.; Murray, J. S.; Politzer, P., *J. Phys. Chem. A* **2007,** *111* (13), 2455.

55. Jaque, P.; Toro-Labbé, A.; Politzer, P.; Geerlings, P., *Chem. Phys. Lett.* **2008,** *456* (4-6), 135.

56. Yepes, D.; Murray, J. S.; Politzer, P.; Jaque, P., *Phys. Chem. Chem. Phys.* **2012,** *14* (31), 11125.

57. Yepes, D.; Donoso-Tauda, O.; Pérez, P.; Murray, J. S.; Politzer, P.; Jaque, P., *Phys. Chem. Chem. Phys.* **2013,** *15* (19), 7311.

58. Rossum, G. V.; Drake, F. L., *Python 3 Reference Manual*. CreateSpace: 2009.

59. Frisch, M. J.; Trucks, G. W.; Schlegel, H. B.; Scuseria, G. E.; Robb, M. A.; Cheeseman, J. R.; Scalmani, G.; Barone, V.; Petersson, G. A.; Nakatsuji, H.; Li, X.; Caricato, M.; Marenich, A.; Bloino, J.; Janesko, B. G.; Gomperts, R.; Mennucci, B.; Hratchian, H. P.; Ortiz, J. V.; Izmaylov, A. F.; Sonnenberg, J. L.; Williams-Young, D.; Ding, F.; Lipparini, F.; Egidi, F.; Goings, J.; Peng, B.; Petrone, A.; Henderson, T.; Ranasinghe, D.; Zakrzewski, V. G.; Gao, J.; Rega, N.; Zheng, G.; Liang, W.; Hada, M.; Ehara, M.; Toyota, K.; Fukuda, R.; Hasegawa, J.; Ishida, M.; Nakajima, T.; Honda, Y.; Kitao, O.; Nakai, H.; Vreven, T.; Throssell, K.; J. A. Montgomery, J.; Peralta, J. E.; Ogliaro, F.; Bearpark, M.; Heyd, J. J.; Brothers, E.; Kudin, K. N.; Staroverov, V. N.; Keith, T.; Kobayashi, R.; Normand, J.; Raghavachari, K.; Rendell, A.; Burant, J. C.; Iyengar, S. S.; Tomasi, J.; Cossi, M.; Millam, J. M.; Klene, M.; Adamo, C.; Cammi, R.; Ochterski, J. W.; Martin, R. L.; Morokuma, K.; Farkas, O.; Foresman, J. B.; Fox, D. J., *Gaussian 16* rev. C. 01; Gaussian Inc.: Wallingford CT.

60. NIST, N., *National Institutes of Standards and Technology, Gaithersburg, MD* **2012**.

61. Virtanen, P.; Gommers, R.; Oliphant, T. E.; Haberland, M.; Reddy, T.; Cournapeau, D.; Burovski, E.; Peterson, P.; Weckesser, W.; Bright, J., *Nat. Methods* **2020,** *17* (3), 261.

62. Woodward, R., *J. Am. Chem. Soc* **1970,** *92*, 7091.

63. Woodward, R., *Angew. Chem* **1969,** *81*, 797.

64. Fleming, I., *Pericyclic reactions*. Oxford University Press, USA: 2015.

65. Ponec, R., *Overlap determinant method in the theory of pericyclic reactions*. Springer Science & Business Media: 2012; Vol. 65.

66. Diels, O.; Alder, K., *Justus Liebigs Ann. Chem* **1928,** *460*, 98.

67. Fernandez, I.; P Cossio, F., *Current Organic Chemistry* **2010,** *14* (15), 1578.

68. von Ragué Schleyer, P.; Wu, J. I.; Cossío, F. P.; Fernández, I., *Chem. Soc. Rev.* **2014,** *43* (14), 4909.

69. Yepes, D.; Valenzuela, J.; Martínez-Araya, J. I.; Pérez, P.; Jaque, P., *Phys. Chem. Chem. Phys.* **2019,** *21* (14), 7412.

70. Glendening, E.; Reed, A.; Carpenter, J.; Weinhold, F., *Theoretical Chemistry Institute, University of Wisconsin, Madison, WI* **1990**.

71. Cui, C. X.; Liu, Y. J., *J. Phys. Org. Chem.* **2014,** *27* (8), 652.

72. Houk, K. N.; Li, Y.; Evanseck, J. D., *Angew. Chem., Int. Ed. Engl.* **1992,** *31* (6), 682.

73. Mandal, D. K., *Pericyclic Chemistry: Orbital Mechanisms and Stereochemistry*. Elsevier: 2018.

74. Wiest, O.; Houk, K.; Black, K.; Thomas IV, B., *J. Am. Chem. Soc.* **1995,** *117* (33), 8594.

75. Doering, W. v. E.; Toscano, V.; Beasley, G., *Tetrahedron* **1971,** *27* (22), 5299.

76. Politzer, P.; Murray, J. S.; Jaque, P., *J. Mol. Model.* **2013,** *19* (10), 4111.

77. Fernández, I.; Sierra, M. A.; Cossío, F. P., *J. Org. Chem.* **2007,** *72* (4), 1488.